Extended Hamilton's principle applied to geometrically exact Kirchhoff sliding rods

Frédéric Boyer, Vincent Lebastard, Fabien Candelier, Federico Renda

Available online at www.sciencedirect.com

ScienceDirect

Journal of Sound and Vibration 00 (2022) 1–29

Journal of Sound and Vibration

Extended Hamilton's principle applied to geometrically exact Kirchhoff sliding rods

Frédéric Boyer[a], Vincent Lebastard[a], Fabien Candelier[b], Federico Renda[c]

[a] *F. Boyer and V. Lebastard are with the LS2N lab, Institut Mines Telecom Atlantique, 44307 Nantes, France. e-mail: frederic.boyer@imt-atlantique.fr, vincent.lebastard@imt-atlantique.fr.*

[b] *F. Candelier is with Aix Marseille Univ., CNRS, IUSTI, Marseille, France. e-mail: fabien.candelier@univ-amu.fr.*

[c] *F. Renda is with the Khalifa University Center for Autonomous Robotics Systems, Khalifa University of Science and Technology, Abu Dhabi, UAE. e-mail: federico.renda@ku.ac.ae.*

Abstract

This article addresses the dynamic modelling of geometrically exact sliding Cosserat rods. Such systems need to consider non-material time-varying domains to which the Lagrangian view point of solid mechanics is inappropriate. In the article here presented, we use the geometrically exact model of inextensible Kirchhoff rods along a non-material domain whose time variations are not necessarily imposed but are governed by the dynamics, i.e. depend on the configuration of the rod. To progress through derivation, we use the variational calculus on Lie group introduced by Poincaré, and apply it to an extension of Hamilton's principle holding for open rod systems, which is derived in the article. This extended variational principle uses a moving non-material tube across which the material rod slides. The resulting closed formulation of sliding rods dynamics takes the form of a set of non-material Cosserat-Poincaré's partial differential equations governing the time-evolution of the cross-section pause of the non-material tube, coupled with an ordinary Lagrange's differential equation for the sliding motion of the rod across the tube. While emphasize is on the dynamic formulations, the modelling approach is numerically illustrated on a few examples related to the so called sliding spaghetti problem.

Keywords: Axially moving beams, Sliding rods, Extended Hamilton's principle, Finite deformations, Geometrically exact beam theory

1. Introduction

Axially moving strings and membranes modelling tapes, belts or other paper rolls subjected to fast large axial motion and small transversal deformations have been studied by mechanical engineers for a long time [1]. A similar situation occurs in robotics when one considers flexible multibody systems containing links that transversally deform while axially sliding through prismatic joints [2]. With the growth of space satellite deployable systems [3], researchers started to address the challenging issue of rods subjected to axial sliding motion and transversal deformations of finite magnitude. Remarkably, this issue has been stated for the first time as an abstract problem in applied mathematics by Carrier [4], through its famous "spaghetti problem", an experience that can be done in everyday life, where we all observed that sucking quickly a spaghetti, generates a slapping motion of increasing bending frequency and amplitude. In contrast to usual structural dynamics, all these systems share the property that they need to be modelled and simulated over non-material domains. For instance, the vibrations of a belt axially moving between two rotating wheels (pulleys) can be studied by isolating its material that flows through a fixed non-material volume bounded by the two supports. Applying this idea requires to consider open material systems, i.e. systems having different material particles along time. Moreover, as soon as the belt is materially not homogenous along the axial moving dimension,

the mass within the domain is no longer constant along time. In the case of sliding systems that can be deployed and retrieved as the sliding spaghetti of Carrier, isolating the part of the rod outside the guide is a natural choice that also leads to consider an open material system with variable mass. In this context, several approaches have been proposed to model these systems as for instance those proposed in [5], [6], [7], [8], followed by Behdinam and al. [9, 10] to name but a few. In all these studies, the deformation of the rod is approximated through truncated expansions, while the axial sliding motion is mostly kinematically imposed along time. In this latter context, it is possible to derive the governing equations of the transversal motions through Newton's law [8] or with an extension of Hamilton's principle to open systems, originally proposed by McIver [11]. Applying the full nonlinear model of Reissner's beams with the geometrically exact finite element method (GE-FEM) of Simo and Vu-Quoc [12], these approximations of deformations were definitely removed in the seminal article of Vu-Quoc and Li [13]. Devoted to modelling and simulation of sliding rods subjected to finite deformations, this extensive framework proposed two modelling approaches. One is a pure Lagrangian approach, in which the axial and transversal motions are not separated thanks to the use of a unique material reference configuration and a stretch coordinate transformation changing the variable domain in a fixed one, over which Reissner's partial differential equations (PDEs) can be pulled back. The second is an Eulerian-Lagrangian approach based on the use of an intermediate sliding configuration with respect to which the transversal deformations are described. Note that this second approach can be embedded in the wider context of the Arbitrary Lagrangian-Eulerian (ALE) nowadays developed in the field of computational fluid-structure interactions [14]. Though decisive, the results of [13] still consider some imposed sliding kinematics. This constraint has been removed in a further important step done by Humer in [15]. In this approach, the Kirchhoff (i.e."shear less") model is used to address the more general context of rods with non-material deformation-dependent boundary conditions. In contrast to most of the above mentioned works, the sliding motion of [15] is no longer imposed but governed by further dynamics that are derived and numerically solved with the GE-FEM. Referred by the author as the "extended sliding spaghetti problem", this full problem allows feeding the sliding dynamics through force and not prescribed motions as this was mostly the case in the past literature. This approach, which uses the stretching coordinate transformation of [13], has been successfully compared to the three-dimensional FEM in [16], and more recently exploited to produce a general GE-FEM able to cope with any set of variable domains in [17].

In the present article, we address the emblematic case of a sliding rod moving in and out of a rigid guide inside a wall. To this end, we reconsider the approach of [9] based on the extension of Hamilton principle to open (non-material) systems. However, in contrast to [9], the model of the rod is geometrically exact and the sliding motion is not constrained by some imposed time-laws but rather governed by dynamics that are derived in the article. To achieve this goal, we use the model of inextensible Kirchhoff rods as a sub-model of the full Cosserat rods theory of Reissner [18], where the non-shear and non-stretch constraints are forced through a set of Lagrange multipliers. As in [9], we first consider the open system constituted by the outer part of the rod enclosed in a non-material volume, a tube, to which extended Hamilton's principle is applied. Inspired from fluid mechanics, this approach allows ignoring the difficulties of modelling the system inside the wall, an advantage which can be particularly useful when considering complex systems such as a cable wound around a roller system for instance. However, since the sliding motion is not imposed, one needs to use a more general version of Hamilton's principle than that proposed in [11]. This further version has been proposed for a classical (not Cosserat) three dimensional medium in [19], and earlier applied in the context of Cosserat rods to Lighthill's large amplitude elongated body theory of fish swimming in [20]. In this other context, the open system includes the fluid and the fish enclosed in a non-material volume that moves with the fish slender body, a choice which allows the complex modelling of the vortical wake to be ignored [21]. As a consequence of the non-material character of the isolated domain, the partial differential equations that govern the time-evolution of the pause field in $SE(3)$ along the non-material tube, take the usual form of the Cosserat-Poincaré PDEs [22], but in a new (non-material) form where the usual time-derivatives are replaced by total derivatives. Note that these equations stand for the planar Eulerian-Lagrangian formulation of [13] but in three dimensions, and with no shear nor stretch. As regards the dynamics of the sliding motion, owing to the inextensibility constraint, they are modelled by an ordinary differential equation (ODE), which contains unusual contributions modelling the transport of the Lagrangian density and its conjugate momenta across the non-material boundaries. In a further step, the approach is extended to the dynamics of the part of the rod inside the rigid guide. This extension, which corresponds to the "extended sliding spaghetti problem" of [15], provides an alternative and simpler way to capture the ODE governing the sliding motion. Moreover, it allows to validate the application of extended Hamilton's principle to this class of

systems. The approach is developed in the context of the variational calculus on Lie groups (here $SE(3)$), a research field historically introduced by Poincaré [23] and developed by Arnold [24] and the geometric mechanics school after Marsden [25]. It is illustrated through several numerical examples related to the retrieval and deployment of slender structures. These simulations are performed with a geometrically exact numerical method recently validated against the GE-FEM of [26], in [27]. It is based on the reduction of the strain fields on a basis of Ritz functions, and the use of an inverse dynamics algorithm directly deduced from the strong formulation of the dynamics.

The article is structured as follows. In section 2, we start by reminding some basic definitions and notations of rigid body mechanics that will be used throughout the article. After a brief introduction to the nonlinear kinematics of Cosserat rods, Section 3 presents the derivation of their dynamic model in the usual case of a non-sliding rod. The approach is based on Hamilton's principle in material variables. This variational calculus is first achieved for the full model of Reissner's beams, and then for the reduced one of inextensible Kirchhoff rods. In section 4, an extended version of Hamilton's principle proved in Appendix B is applied to the non-material case of the outer part of an inextensible Kirchhoff rod sliding out of a rigid guide. The weak form deduced from this variational principle provides a closed dynamic formulation of the system in the form of a new set of non-material Poincaré equations coupled to non-material Lagrange's ones (section 5). In section 6, the approach is extended to the entire rod, including its inner part. While essentially focused on theoretical aspects, the article continues with some numerical applications of the approach to several cases related to the sliding spaghetti problem in section 7. Finally, the article ends with a few concluding remarks (section 8).

2. Basic definitions and notations of rigid body mechanics

Throughout the article, a hat "$\wedge$" covering a vector Υ defines a matrix $\hat{\Upsilon} = \Upsilon^{\wedge}$ whose definition depends on the dimension of Υ. Namely, if $\Upsilon \in \mathbb{R}^3$, $\hat{\Upsilon}$ denotes the unique 3×3 skew-symmetric matrix such that $\hat{\Upsilon}V = \Upsilon \times V$ for any $V \in \mathbb{R}^3$. If $\Upsilon = (W^T, U^T)^T \in \mathbb{R}^6$, with W and U two any (column) vectors of $\mathbb{R}^3$, then $\hat{\Upsilon}$ is the unique 4×4 matrix defined by:

$$\hat{\Upsilon} = \begin{pmatrix} \hat{W} & U \\ 0_{1\times 3} & 0 \end{pmatrix}. \tag{1}$$

Reciprocally the superscript "$\vee$" (anti-hat), is such that $\hat{\Upsilon}^{\vee} = \Upsilon$ for any Υ in $\mathbb{R}^3$ or $\mathbb{R}^6$. For the sake of concision, we use a very few of the Lie group definitions of [25], that we now remind. The transformations applied to a rigid body can be represented by 4×4 homogenous matrices of the form:

$$g = \begin{pmatrix} R & r \\ 0_{1\times 3} & 1 \end{pmatrix}, \tag{2}$$

where R is a 3×3 rotation matrix (i.e. an element of $SO(3)$), and $r \in \mathbb{R}^3$ is a translation vector. The matrices (2) can be used in all the expressions of the article, while in the text, we will sometimes note in a more concise way $g = (R, r)$. Geometrically, the g matrices define the pauses of a mobile frame attached to the body with respect to a fixed inertial frame, and more abstractly, points on the non-commutative Lie group $SE(3)$. The velocities of a rigid body define the Lie algebra of $SE(3)$, denoted $se(3)$, which is here represented by the space of twists, i.e. by 6×1 vectors $\eta = (\Omega^T, V^T)^T$ composed of an angular component Ω (angular velocity) and a linear one V (linear velocity). The space of twists is endowed with a Lie bracket $[.,.]$, defined for any pair $\eta_1 = (\Omega_1^T, V_1^T)^T$ and $\eta_2 = (\Omega_2^T, V_2^T)^T$, by:

$$[\eta_1, \eta_2] = ad_{\eta_1}\eta_2, \tag{3}$$

where we introduced the operator $ad_{.}$, defined for any $\Upsilon = (W^T, U^T)^T$, with $W, U \in \mathbb{R}^3$, by the 6×6 matrix:

$$ad_{\Upsilon} = \begin{pmatrix} \hat{W} & 0_{3\times 3} \\ \hat{U} & \hat{W} \end{pmatrix}. \tag{4}$$

Based on these definitions, $se(3)$ is represented by $\mathbb{R}^6$ endowed with the ad operator. The dual space of twists, noted $se(3)^{\star}$, is the space of wrenches that model the forces experienced by a rigid body. Like twists, wrenches are 6×1

vectors $F = (C^T, N^T)^T$ composed of an angular component C (a torque) and a linear one N (a force). Using the $\wedge$ and $\vee$ operators, one can link twists η to transformations g, through the two equivalent relations:

$$\eta = (g^{-1}\partial_t g)^\vee \quad , \quad \partial_t g = g\hat{\eta}, \tag{5}$$

where t typically represents time, while Ω and V of $\eta = (\Omega^T, V^T)^T$, stand for the angular and linear velocity of the body expressed in its mobile frame (taking $\eta = (\partial_t g g^{-1})^\vee$ an $\partial_t g = \hat{\eta} g$, instead of (5), would define them as expressed in the fixed (inertial) frame). Note that the vector space of matrices $\hat{\eta}$ defined by (5), is another representation of $se(3)$ whose Lie bracket is the usual commutator of matrices $[\hat{\eta}_1, \hat{\eta}_2] = \hat{\eta}_1\hat{\eta}_2 - \hat{\eta}_2\hat{\eta}_1$, and we have the relation between this commutator and the Lie bracket of twists:

$$[\hat{\eta}_1, \hat{\eta}_2]^\vee = ad_{\eta_1}\eta_2. \tag{6}$$

For practical computations, we will extensively use the canonical basis $(\mathbb{E}_1, \mathbb{E}_2, \mathbb{E}_3, \mathbb{E}_4, \mathbb{E}_5, \mathbb{E}_6)$ of $\mathbb{R}^6$ identified to the Lie algebra of twists and wrenches, with $\mathbb{E}_1 = (E_1^T, 0_{1\times3})^T$, $\mathbb{E}_2 = (E_2^T, 0_{1\times3})^T$, $\mathbb{E}_3 = (E_3^T, 0_{1\times3})^T$, $\mathbb{E}_4 = (0_{1\times3}, E_1^T)^T$, $\mathbb{E}_5 = (0_{1\times3}, E_2^T)^T$ and $\mathbb{E}_6 = (0_{1\times3}, E_3^T)^T$, and where (E_1, E_2, E_3) is the canonical (numerical) basis of $\mathbb{R}^3$, with $E_1 = (1,0,0)^T$, $E_2 = (0,1,0)^T$, $E_3 = (0,0,1)^T$. Finally, all these concepts of rigid body mechanics will be applied to the rigid cross-sections of a rod, and except in one single remark (numbered 6), all the expressions of the article can be interpreted as matrix relations in terms of components in the mobile basis of the cross-sectional frames. In this context, the *ad* operator will be used to encode the contribution of the time, and space derivatives of the cross sectional basis vectors, when deriving a vector with respect to the inertial frame.

3. Reminders about Cosserat rods

In the language of continuum mechanics [28], a Cosserat rod is a one-dimensional continuum of rigid cross sections. In this section, we will first recall how the concepts of section 2 apply to such a medium. Based on these preliminaries, we will consider two models of Cosserat rods, called Reissner [18] and Kirchhoff [29] models, depending on whether or not transverse shear and stretch is considered. The Reissner model is the most general Cosserat rod model, and sometimes referred to as the "full Cosserat" model in the article. As such, it can be derived from Hamilton's principle by direct application of the variational calculation on $SE(3)$. To benefit from the same calculation for Kirchhoff's model, we will use an augmented Lagrangian formulation, with a set of Lagrange multipliers forcing shear and stretch to zero into the Reissner model. In this section, all these investigations are performed step by step in the usual material context of non-sliding rods, and prepare their generalization to sliding rods (in sections 4, 5 and 6).

3.1. Cosserat rod kinematics

We here consider an elastic beam of constant circular cross-section along its length. The radius of its cross-sections is denoted by a, while ρ, E and G denote its volume mass, its Young modulus and its shear modulus respectively. This rod is subjected to finite displacements and small strains. In the Cosserat approach, such a medium is modeled by a continuous set of rigid cross sections stacked along a material line parameterized by a coordinate X which plays the role of a continuous label for the cross sections. A natural choice for X that we here adopt, consists in defining it as the arc length of the rod in its reference (at rest) configuration. If l denotes the length of the rod in such a configuration, we then have $X \in [0, l]$. To each X-cross section, a mobile cross-sectional frame $\mathcal{F}(X) = (O, t_1, t_2, t_3)(X)$ is attached, where $O(X)$ and $t_1(X)$ coincide with the center of the cross section and its unit normal vector, respectively. In this context, the configuration of any cross section is defined by the action of an element of $g \in SE(3)$ on a unique inertial frame $\mathcal{F}_s$. In details, $g(X) = (R, r)(X)$, where $R(X) \in SO(3)$, and $r(X) \in \mathbb{R}^3$, are the orientation (or rotation) matrix of $\mathcal{F}(X)$, and the position vector of $O(X)$ in $\mathcal{F}_s$, respectively. Hence, the beam configuration space is naturally defined as:

$$C = \{g(.) : X \in [0, l] \mapsto g(X) \in SE(3)\}, \tag{7}$$

which stands for a functional space of curves in $SE(3)$. Throughout the article, partial derivatives $\partial./\partial X$ and $\partial./\partial t$ are indicated by ∂_X and ∂_t, respectively. The field g depending on both X and t, its space-time variations can be entirely described by the two vector fields η and ξ from $[0, l]$ to $se(3) \cong \mathbb{R}^6$:

$$\eta = (g^{-1}\partial_t g)^\vee \, , \, \xi = (g^{-1}\partial_X g)^\vee, \tag{8}$$

where $\eta = (\Omega^T, V^T)^T$ stands for the field of the velocity twists of the cross-sections in their mobile frames with $\Omega = (\Omega_1, \Omega_2, \Omega_3)^T \in \mathbb{R}^3$ and $V = (V_1, V_2, V_3)^T \in \mathbb{R}^3$, the angular and linear velocity field, while $\xi = (K^T, \Gamma^T)^T$ is the exact geometrical counterpart of η when replacing t by X. In particular, $K(X) = (K_1, K_2, K_3)^T(X) \in \mathbb{R}^3$ is the vector of twisting (K_1) and curvatures (K_2 and K_3) of the rod at X. Any objective strain tensor has to depend on the current configuration g through the field ξ only [22]. For instance, if g_o defines a stress-free reference configuration of the beam, a linear strain field is simply provided by $\epsilon = \xi - \xi_o$ with $\xi_o = (g_o^{-1} g_o')^\vee = (K_o^T, E_1^T)^T$ and $K_o = (0, K_{o,2}, K_{o,3})^T$. The velocity and strain fields η and ξ have their dual counterparts in $se(3)^\star \cong \mathbb{R}^6$. Denoted $\Sigma = (\Upsilon^T, P^T)^T$ and $\Lambda = (C^T, N^T)^T$, these two further fields of wrench model the cross-sectional kinetic momenta and stress along the beam respectively, where $C = (C_1, C_2, C_3)(X)^T \in \mathbb{R}^3$ and $N = (N_1, N_2, N_3)(X)^T \in \mathbb{R}^3$ denote the couple stress and the resultant of stress forces exerted by the right piece of rod onto the left part across the X-cross section.

3.2. Reissner rod dynamics

Based on the model of Cosserat rods, some constraints can be imposed to the internal rod kinematics as for instance its inextensibility or unshearability. In the most general case, the six scalar fields of ξ are free and related to the six stress scalar fields of Λ through a constitutive law, which in the case of the small strains assumption, takes the linear Hookean form:

$$\Lambda = \mathcal{H}(\xi - \xi_o), \tag{9}$$

where $\mathcal{H} = \text{diag}(\mathcal{H}_a, \mathcal{H}_l) \in \mathbb{R}^6 \otimes \mathbb{R}^6$, is the cross-sectional Hooke tensor field along the rod, with $\mathcal{H}_a = \text{diag}(GJ_1, EJ_2, EJ_3)^T$ and $\mathcal{H}_l = \text{diag}(EA, GA, GA)^T$, the angular and linear Hooke tensor, with $A = \pi a^2$, $J_1 = 2J_2 = 2J_3 = \pi a^4/2$. Applying Hamilton's principle in this geometric context, provides the dynamic model of Reissner rods. This principle can be stated as follows. Among all trajectories virtually accessible to the rod between two fixed times t_a and t_b, the real trajectory it will actually follow must satisfy the stationarity condition which imposes that for any $\delta\zeta = (g^{-1}\delta g)^\vee \in se(3) \cong \mathbb{R}^6$, such that $\delta\zeta(t_a) = \delta\zeta(t_b) = 0$, one has:

$$\delta \int_{t_a}^{t_b} \int_0^l \mathfrak{L}\, dX\, dt = - \int_{t_a}^{t_b} \delta W_{ext}\, dt, \tag{10}$$

where $\mathfrak{L}$ is the Lagrangian density of the rod (reduced in the Lie algebra $se(3)$), which takes the form:

$$\mathfrak{L}(\eta, \xi) = \frac{1}{2}\eta^T \mathcal{M}\eta - \frac{1}{2}(\xi - \xi_o)^T \mathcal{H}(\xi - \xi_o), \tag{11}$$

with $\mathcal{M} = \text{diag}(\rho J, \rho A 1_{3\times 3}) \in \mathbb{R}^6 \otimes \mathbb{R}^6$, the cross-sectional inertia tensor field in which $J = \text{diag}(J_1, J_2, J_3)$, while δW_{ext} stands for the virtual work of external forces, which in the case of a rod kinematically free at its two tips, takes the general form:

$$\delta W_{ext} = \int_0^l \delta\zeta^T \bar{F}_{ext}\, dX + \delta\zeta^T(0) F_{ext}^- + \delta\zeta^T(l) F_{ext}^+, \tag{12}$$

where the rod is subjected to a density of state-dependent external wrench $\bar{F}_{ext} = (\bar{C}_{ext}^T, \bar{N}_{ext}^T)^T$ on $]0, l[$ and possibly to two tip external wrenches $F_{ext}^- = ((C_{ext}^-)^T, (N_{ext}^-)^T)^T$ and $F_{ext}^+ = ((C_{ext}^+)^T, (N_{ext}^+)^T)^T$ at $X = 0$ and $X = l$ respectively. To apply the common uses of variational calculus to the functional of (10), one needs first to impose the constraints of variation at fixed time, and fixed material label (see Appendix A):

$$\delta\eta = \partial_t \delta\zeta + ad_\eta \delta\zeta \ , \ \delta\xi = \partial_X \delta\zeta + ad_\xi \delta\zeta \ . \tag{13}$$

Then, introducing (13) in (10), and achieving usual space-time by part integration, provides the weak form of virtual works:

$$\int_0^l \delta\zeta^T \left(\frac{\partial}{\partial t}\left(\frac{\partial \mathfrak{L}}{\partial \eta}\right) - ad_\eta^T \left(\frac{\partial \mathfrak{L}}{\partial \eta}\right) + \frac{\partial}{\partial X}\left(\frac{\partial \mathfrak{L}}{\partial \xi}\right) - ad_\xi^T \left(\frac{\partial \mathfrak{L}}{\partial \xi}\right) - \bar{F}_{ext} \right) dX \tag{14}$$

$$= \left[\delta\zeta^T(X) \left(\frac{\partial \mathfrak{L}}{\partial \xi}\right)(X) \right]_0^l + \delta\zeta(0)^T F_{ext}^- + \delta\zeta(l)^T F_{ext}^+, \tag{15}$$

which holds for any $\delta\zeta$ compatible with the possible geometric boundary conditions (BCs). In the case of a rod kinematically free at its two ends, $\delta\zeta(.)$ on $]0, l[$ and $\delta\zeta(0)$, $\delta\zeta(l)$, can be considered as independent in (15), and one obtains

the closed dynamic formulation in the form of its Cosserat-Poincaré partial differential equations (PDEs) [22]:

• PDEs of $g(.)$:

$$\frac{\partial}{\partial t}\left(\frac{\partial \mathfrak{Q}}{\partial \eta}\right) - ad_{\eta}^{T}\left(\frac{\partial \mathfrak{Q}}{\partial \eta}\right) + \frac{\partial}{\partial X}\left(\frac{\partial \mathfrak{Q}}{\partial \xi}\right) - ad_{\xi}^{T}\left(\frac{\partial \mathfrak{Q}}{\partial \xi}\right) = \bar{F}_{ext}. \tag{16}$$

• BCs:

$$\left(\frac{\partial \mathfrak{Q}}{\partial \xi}\right)(0) = F_{ext}^{-}\ ,\ \left(\frac{\partial \mathfrak{Q}}{\partial \xi}\right)(l) = -F_{ext}^{+}. \tag{17}$$

• Reconstruction equations:

$$\partial_t g = g\hat{\eta}. \tag{18}$$

• Constitutive law:

$$\left(\frac{\partial \mathfrak{Q}}{\partial \xi}\right) = -\mathcal{H}(\xi - \xi_o). \tag{19}$$

Introducing (11) into (16-19) provides the detailed formulation:

• PDEs of $g(.)$:

$$\mathcal{M}\partial_t \eta - ad_{\eta}^{T}\mathcal{M}\eta - \partial_X \Lambda + ad_{\xi}^{T}\Lambda = \bar{F}_{ext}. \tag{20}$$

• BCs:

$$\Lambda(0) = -F_{ext}^{-}\ ,\ \Lambda(l) = F_{ext}^{+}. \tag{21}$$

• Reconstruction equations:

$$\partial_t g = g\hat{\eta}. \tag{22}$$

• Constitutive law:

$$\Lambda = \mathcal{H}(\xi - \xi_o). \tag{23}$$

Note that (20) is a PDE which governs the time-evolution of η. Hence, it needs to be supplemented with the reconstruction equation (a kinematic model) (18). Finally, the model of Reissner beams [18], is at the basis of the geometrically exact finite element method of [26]. In this numerical context, the weak-form of virtual works (15) is spatially discretized in finite-elements, and solved at each step of a time-loop with respect to a set of nodal velocities. Then the beam configuration is updated by using a discrete version of the reconstruction equation (18), based on the exponential map [26].

3.3. From Reissner to inextensible Kirchhoff rods

In the rest of the article, we will not use the Reissner model but rather that of Kirchhoff inextensible rods, i.e. Cosserat rods whose stretch and shear can be neglected. This assumption is in most of cases justified by the experience. Note that these simplifications only concern the internal kinematics of the rod and not those of its transformations. In short, the model will remain geometrically exact. To capture this further model, we use the augmented Lagrangian which is defined on the full configuration space (7):

$$L = \int_0^l \frac{1}{2}\eta^T \mathcal{M}\eta - \frac{1}{2}(K - K_o)^T \mathcal{H}_a (K - K_o) - (\Gamma - E_1)^T N\, dX, \tag{24}$$

where from left to right, one finds the density of kinetic energy of the rod, its density of internal strain energy, and an additional density of potential energy in charge of forcing through a field of internal forces N (Lagrange multipliers), the no-stretch nor shear constraint, which with our notations takes the form:

$$\Gamma = E_1. \tag{25}$$

Now remark that (24) takes the form:

$$L = \int_0^l \mathfrak{Q}(\eta, \xi, N)\, dX. \tag{26}$$

Applying Hamilton's principle (10) to this augmented Lagrangian with $(g, N)(.)$ considered as two independent fields, gives for a rod kinematically free at its two tips:

$$\int_{t_a}^{t_b}\left(\int_0^l \delta\eta^T\left(\frac{\partial\mathfrak{L}}{\partial\eta}\right)+\delta\xi^T\left(\frac{\partial\mathfrak{L}}{\partial\xi}\right)+\delta N^T\left(\frac{\partial\mathfrak{L}}{\partial N}\right)dX\right)dt=-\int_{t_a}^{t_b}\left(\int_0^l \delta\zeta^T\bar{F}_{ext}\,dX+\delta\zeta^T(0)F_{ext}^-+\delta\zeta^T(l)F_{ext}^+\right)dt. \quad (27)$$

Then, using the commutation relations (13) and standard variational calculus at fixed time-ends, one obtains the weak form:

$$\int_0^l \delta\zeta^T\left(\frac{\partial}{\partial t}\left(\frac{\partial\mathfrak{L}}{\partial\eta}\right)-ad_\eta^T\left(\frac{\partial\mathfrak{L}}{\partial\eta}\right)+\frac{\partial}{\partial X}\left(\frac{\partial\mathfrak{L}}{\partial\xi}\right)-ad_\xi^T\left(\frac{\partial\mathfrak{L}}{\partial\xi}\right)-\bar{F}_{ext}\right)dX$$
$$-\int_0^l \delta N^T\left(\frac{\partial\mathfrak{L}}{\partial N}\right)dX=\left[\delta\zeta^T(X)\left(\frac{\partial\mathfrak{L}}{\partial\xi}\right)(X)\right]_0^l+\delta\zeta(0)^TF_{ext}^-+\delta\zeta(l)^TF_{ext}^+, \quad (28)$$

which needs to be satisfied for any δN, and for any $\delta\zeta$ compatible with the Reissner rod kinematics and the geometric boundary conditions (BCs). For instance, considering an inextensible Kirchhoff rod kinematically free at its two ends, the weak form (28) provides Cosserat-Poincaré equations similar to (16-18), but with constitutive law and constraints:

$$\left(\frac{\partial\mathfrak{L}}{\partial K}\right)=-\mathcal{H}_a(K-K_o)\,,\ \left(\frac{\partial\mathfrak{L}}{\partial N}\right)=0\,. \quad (29)$$

Now, detailing the Lagrangian density of (24) as $\mathfrak{L}=\mathfrak{T}-\mathfrak{U}$ with:

$$\mathfrak{T}(\eta)=\frac{1}{2}\eta^T\mathcal{M}\eta\quad,\quad \mathfrak{U}(\xi,N)=\frac{1}{2}(K-K_o)^T\mathcal{H}_a(K-K_o)+(\Gamma-E_1)^TN, \quad (30)$$

one can define the field of stress wrench:

$$\frac{\partial\mathfrak{U}}{\partial\xi}=\Lambda=\begin{pmatrix}C\\N\end{pmatrix}=\begin{pmatrix}\mathcal{H}_a(K-K_o)\\N\end{pmatrix}. \quad (31)$$

Using these definitions in the Cosserat-Poincaré equations, they can be still detailed as (20-22), but with the constitutive law and constraint:

$$C=\mathcal{H}_a(K-K_o)\,,\ \Gamma=E_1\,. \quad (32)$$

Finally, it is worth noting that once the variational calculus achieved, the dynamics of an inextensible Kirchhoff rod can be easily deduced from those of a Reissner rod. Indeed, it suffices to force the relation $\Gamma=E_1$, and to replace the full constitutive law (9) by the reduced one (32) in Reissner's model.

Remark 1: Note here that (25) modeling ideal kinematics constraints, it can be interpreted as a constitutive law for (N,Γ), i.e. one can formulate the last equation of (29) as:

$$N \text{ s.t. } \Gamma-E_1=0\,. \quad (33)$$

Remark 2: Using the above model, it is quite straightforward to derive the closed dynamic formulation of a non sliding rod fixed to a wall at its root but able to rotate around the normal to its support with a prescribed axial external torque $\mathbb{E}_1^TF_{ext}^-=C_{ext,1}^-(t)$, while being kinematically free at the other end. To that end, it suffices to develop the weak form (28) with a virtual displacement compatible with the geometric BC at the root:

$$r(0)=0\quad,\quad R(0)E_1=e_1, \quad (34)$$

i.e, with a field $\delta\zeta$ such that:

$$\delta\zeta(0)=\delta\zeta_1(0)\mathbb{E}_1. \quad (35)$$

Such a formulation reads:

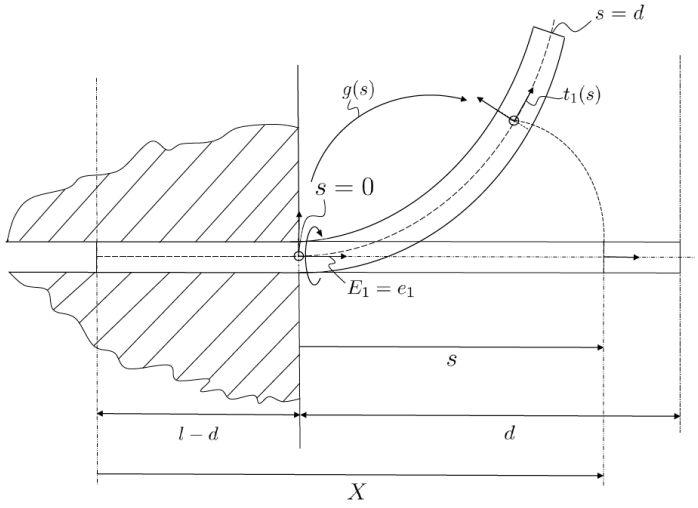

Figure 1. Parametrization of the sliding rod.

• PDEs of $g(.)$:

$$\mathcal{M}\partial_t\eta - ad_\eta^T\mathcal{M}\eta - \partial_X\Lambda + ad_\xi^T\Lambda = \bar{F}_{ext}. \tag{36}$$

• BCs:

$$r(0) = 0\ ,\ R(0)E_1 = e_1\ ,\ \mathbb{E}_1^T\Lambda(0) = -C_{ext,1}^-\ ,\ \Lambda(l) = F_{ext}^+. \tag{37}$$

• Reconstruction equations:

$$\partial_t g = g\hat{\eta}. \tag{38}$$

• Constitutive law and constraints:

$$C = \mathcal{H}_a(K - K_o)\quad ,\quad \Gamma = E_1\ . \tag{39}$$

We are now ready to extend this picture from the material to the non-material context. To that end, we will re-use the model of an inextensible Kirchhoff rod, but will replace the material abscissa X by a geometric (non-material) one, noted s, which is adapted to the context of sliding rods.

4. Extended Hamilton's principle applied to a sliding rod

In the rest of the article, one considers a single inextensible Kirchhoff rod of total length l, sliding through a straight rigid guide across a vertical wall. In a first step (sections 4 and 5), we ignore the part of the rod inside the wall, and focus our attention on its outer part only. The rod is then subjected to an axial force which pushes or pulls it across the wall, as well as a rolling torque, both imposed at the root of the rod in the wall through a sliding-pivot joint normal to it as in remark 2. This external rod is subjected to other state-dependent external forces, that to fix the ideas, we assume to be reduced to the gravity volume forces distributed along the rod, and to a possible concentrated wrench at the kinematically free tip of the rod (e.g. imposed by its contact with the environment). This context is summarized in figure 1. We are interested in the derivation of a closed formulation of the dynamics of the part of the rod deployed at each instant out of the wall. To model such a system we first enclose it in an one-dimensional non-material domain (a tube), whose boundaries follow the deployed part of the rod in space. The material system isolated at each time in such a tube defines an open system, i.e. a system which is not constituted of the same material particles along time, and that not only can exchange energy with the rest of the world, but also mass. To derive the Lagrangian dynamics of such a system, we apply the extended Hamilton principle for open system proposed in [20], that is here instantiated to sliding Cosserat rods. To introduce this approach, we first present a kinematic model of such an open system.

4.1. Basic kinematic picture

At each instant, the rod configuration is parameterized by the field of pose of the cross-sections of the non-material tube that coincides with the outer part of the real rod. This field is defined as $g(.) : s \in [0, d] \mapsto g(s) \in SE(3)$, where s is the arc length along the non-material tube, and d is the deployed rod length. Thus, we use as configuration space:

$$\begin{aligned} C = \{(g(.), d),\ \text{with: } d \in \mathbb{R},\ \text{and: } g(.) : s \in [0, d] \mapsto g(s) \in SE(3), \\ \text{with: } g(0) \text{ s.t. } r(0) = 0, R(0)E_1 = e_1\}, \end{aligned} \tag{40}$$

where the constraints $R(0)E_1 = e_1$ and $r(0) = 0$, translate the fact that at its root on the wall, the rod cannot only slide along its axis but also rotate around it. It is worth noting that in contrast to (7), the field $g(.)$ in the definition (40) depends on a variable s which does not coincide with the Lagrangian label X of the material cross-sections but is rather related to it by the relation:

$$X \in [\underline{X}, l] \mapsto s(X, d) = X + d - l \in [0, d], \tag{41}$$

where $\underline{X} = l - d$ is the label of the cross section lying in the wall plane at the root (see figure 1). To recover the link with true material particles, while using functions of s, one can resort to the standard definitions of fluid mechanics, and use the real and virtual time-rate of variations of any function of s, while following the X-cross sections. Such differential operators can be named "material" or "total derivative" and "material" or "total variation", respectively, and defined by:

$$\frac{D}{Dt} = \frac{\partial}{\partial t} + \dot{d}\frac{\partial}{\partial s}\ ,\ \Delta = \delta + \delta d\frac{\partial}{\partial s}\ , \tag{42}$$

where $\dot{d}$ and δd are the usual real and virtual time-derivative of the scalar function d. Moreover, owing to (41), we simply have:

$$\frac{\partial}{\partial s} = \frac{\partial}{\partial X}\ . \tag{43}$$

In the following, we will often use the simplified notations:

$$D_t = \frac{D}{Dt}\ ,\ \partial_t = \frac{\partial}{\partial t}\ ,\ \partial_s = \frac{\partial}{\partial s}\ . \tag{44}$$

Applying these definitions to the field of pauses $s \mapsto g(s)$, the twist field of material velocity can be expressed as:

$$\eta_{_D} \triangleq \left(g^{-1}D_t g\right)^\vee = (g^{-1}(\partial_t g + \dot{d}\partial_s g))^\vee = (g^{-1}\partial_t g)^\vee + \dot{d}(g^{-1}\partial_s g)^\vee = \eta + \xi\dot{d}\ , \tag{45}$$

while any admissible virtual displacement field needs to be compatible with (45), and so takes the form:

$$\Delta\zeta \triangleq \left(g^{-1}\Delta g\right)^\vee = (g^{-1}(\delta g + \delta d\partial_s g))^\vee = (g^{-1}\delta g)^\vee + \delta d(g^{-1}\partial_s g)^\vee = \delta\zeta + \xi\delta d\ , \tag{46}$$

where we re-used the notations of the Lagrangian (material) context of section 3, i.e. $\eta = (g^{-1}\partial_t g)^\vee$, $\xi = (g^{-1}\partial_s g)^\vee$, and $\delta\zeta = (g^{-1}\delta g)^\vee$, but with $g(.)$ now defined as a s-dependent field.

Remark 3: Note that the context above has a simple kinematic interpretation. Indeed, the space of X-material cross sections and that of s-non-material ones, coincide at each time but due to sliding, move with different velocities. This is shown by (45), where $\eta_D(s)$ stands for the velocity of the X-cross section that coincides with the s-cross section of velocity $\eta(s)$, while $\xi(s)\dot{d}$ represents the relative sliding component between both cross-sections. In particular, noting $\eta_{_D} = (\Omega_{_D}^T, V_{_D}^T)^T$, $\eta = (\Omega^T, V^T)^T$, with $V_{_D} = (V_{D,1}, V_{D,2}, V_{D,3})^T$, and $V = (V_1, V_2, V_3)^T$, we have the relation:

$$V_{D,1} - V_1 = \dot{d}, \tag{47}$$

which represents the axial (along rod's center-line) relative velocity, between the material and non-material tube-cross sections. Based on this kinematic picture, one can state a one-dimensional version of the Reynolds transport theorem,

which will help us to translate the integral principles of dynamics in terms of the non-material variable s. For any scalar density f defined as a function of s mechanically related to the coincident X-cross section, we have the relation:

$$\frac{D}{Dt}\int_0^d f ds = \frac{d}{dt}\int_0^d f ds + [f(V_{D,1} - V_1)]_0^d = \frac{d}{dt}\int_0^d f ds + [f]_0^d \dot{d}. \tag{48}$$

In this equation, $D./Dt$ measures the time-rate of variation of f integrated over all the material cross-sections contained in $[0, d]$ at a given time t, while following their motion. On the other hand, $d./dt$ measures the time-variation of the same quantity, but following the motion of the tube cross-sections. This kinematic picture also holds for any admissible virtual displacement (46). Therefore, using the variational counterpart of (47):

$$\Delta\zeta_1 - \delta\zeta_1 = \delta d, \tag{49}$$

the counterpart of (48) reads:

$$\Delta\int_0^d f ds = \delta\int_0^d f ds + [f(\Delta\zeta_1 - \delta\zeta_1)]_0^d = \delta\int_0^d f ds + [f]_0^d \delta d. \tag{50}$$

Remark 4: Finally, with our definition (40) of the rod's configurations, its kinematics are split into two components. The first component models the sliding motion of the rod relative to the non-material tube in an Eulerian way. It will be governed by the dynamics of d (in fact $\dot{d}$). The second, models the motion of the tube itself, with respect to the ambient space. It will be described in a Lagrangian way through the dynamics of $g(.)$ ($g(s), \forall s \in [0, d]$). It is worth noting that in this hybrid (Eulerian/Lagrangian) description which is a particular case of the more general ALE [14], the variable $s \in [0, d]$ has a double status. Indeed, for the sliding kinematics, it plays the role of a fixed Eulerian variable over a moving domain $[0, d]$, while for the tube-transformation, i.e. for the dynamics of $g(.)$, it plays the role of an usual Lagrangian label over $[0, d]$ considered as a fixed non-material domain. In particular, as in the usual material setting of section 3, $d./dt$ and $\delta.$ being applied while maintaining s fixed, they can be shifted inside the integral over $[0, d]$ of (48) and (50) respectively. Thus, the above two Reynolds theorems read:

$$\frac{D}{Dt}\int_0^d f ds = \int_0^d \frac{\partial f}{\partial t} ds + [f]_0^d \dot{d} \ , \ \Delta\int_0^d f ds = \int_0^d \delta f ds + [f]_0^d \delta d. \tag{51}$$

Remark 5: Going into further details, the pull-back process which allows to shift from the pure material description (i.e. with a unique field $g(X)$) of section 3, to the hybrid description in terms of $(g(s), d)$, is achieved in two steps. In the first step, one replaces all the X-dependent fields by their s-dependent counterparts through the change of variable (41), while the usual δ and ∂_t operators at X fixed of the material (Lagrangian) context, are replaced by D_t and Δ, which represent the same operators, but applied to functions of s and t. This first step is Eulerian and applied to describe the sliding motion of the rod across the tube without resorting to any reference configuration. The second step is Lagrangian and describes the motion of the tube considered as a fictitious "non-material rod" with reference configuration, the reference configuration of the piece of rod deployed out of the wall at the current time. Technically, once the first step is achieved, the formulation only handles s-dependent fields with differential operators $\delta.$ and ∂_t at s fixed, which all behave as in the standard variational calculus of the (non-sliding) material case of section 3. In the subsequent developments, the rod's dynamics are derived with this hybrid process. This starts by shifting the rod's Lagrangian, from the Lagrangian to this Eulerian/Lagrangian setting.

4.2. Lagrangian of a sliding inextensible Kirchhoff rod

To derive the expected dynamic model from Hamilton's least action principle, we need first to calculate the Lagrangian density. To this end, we start from the definition of the Lagrangian in terms of the material label of the rod in the form of (26,30,31), that we reexpress in terms of the non-material variable s defined by (41). This shifting reads:

$$\begin{aligned} L &= \int_{\underline{X}}^{l} \frac{1}{2}\eta^T \mathcal{M}\eta - \frac{1}{2}(K - K_o)^T \mathcal{H}_a (K - K_o) - (\Gamma - E_1)^T N \, dX \\ &= \int_0^d \frac{1}{2}\eta_D^T \tilde{\mathcal{M}}\eta_D - \frac{1}{2}(K - \tilde{K}_o)^T \tilde{\mathcal{H}}_a (K - \tilde{K}_o) - (\Gamma - E_1)^T N \, ds, \end{aligned} \tag{52}$$

where we used the conventional notation which holds for any field f:

$$f(X) = f(s + l - d) = \tilde{f}(s), \tag{53}$$

and which allows to keep track of the cross-sectional label X for all fields that have an intrinsic material nature, i.e. which are primarily defined on the reference configuration of the rod in terms of X. This is the case of $\mathcal{M}$ which depends on the mass density, and of $\mathcal{H}_a$ and K_o[1]. Assuming the uniformity of $\mathcal{M}$ and $\mathcal{H}_a$ along the rod, we have $\tilde{\mathcal{M}} = \mathcal{M}$ and $\tilde{\mathcal{H}}_a = \mathcal{H}_a$. Next, introducing (45) into (52), defines the Lagrangian density:

$$\mathfrak{L} = \frac{1}{2}\eta_{_D}^T \mathcal{M}\eta_{_D} - \mathfrak{U}(\xi, N) = \frac{1}{2}(\eta + \dot{d}\xi)^T \mathcal{M}(\eta + \dot{d}\xi) - \mathfrak{U}(\xi, N), \tag{54}$$

which takes the generic form depending on fields of the non-material variable s:

$$s \in [0, d] \mapsto \mathfrak{L}(\eta_{_D}, \xi, N) = \mathfrak{L}(\eta + \dot{d}\xi, \xi, N) = \mathfrak{L}(\eta, \xi, \dot{d}, N) \in \mathbb{R}, \tag{55}$$

where note that since $\mathfrak{L}$ depends on η through $\eta_{_D} = \eta + \dot{d}\xi$, we have $\partial\mathfrak{L}/\partial\eta_{_D} = \partial\mathfrak{L}/\partial\eta$. Note that $\mathfrak{L}$ depends on d only through the length of its domain of definition. Moreover, it does not explicitly depend on $g(s)$, since this dependence can only occur because of non-symmetric external forces as gravity. In this later case, although being conservative, these forces are modelled through the virtual work of external forces. Finally, the Lagrangian density and the model of external forces are the only ingredients required by the variational principle which we will now detail.

4.3. Hamilton's principle for a sliding rod

Now let us consider the material system contained in the volume tube $[0, d]$. Owing to its open nature, we need to apply an extended version of Hamilton's principle first used in [20] for modelling a swimming slender body, and more recently derived in the general case of a classical (not "Cosserat") medium by Casseta and Pesce [19]. Note that this extension generalizes the version originally proposed in [11]. This extended principle is here specialized to our sliding inextensible Cosserat rod, and takes the form (see Appendix B):

$$\int_{t_a}^{t_b} \left(\int_0^d \delta\mathfrak{L}\, ds + [\mathfrak{L}]_0^d\, \delta d \right) dt - \int_{t_a}^{t_b} \left(\left[\Delta\zeta^T \left(\frac{\partial \mathfrak{L}}{\partial \eta} \right) \right]_0^d \dot{d} - \Delta W_{ext} \right) dt = 0, \tag{56}$$

which much holds for any independent variations $(\delta\zeta(.), \delta N(.), \delta d)$ compatible with the internal rod kinematics and the geometric boundary conditions, and such that $\delta\zeta(., t_a) = \delta\zeta(., t_b) = 0$ and $\delta d(t_a) = \delta d(t_b) = 0$. In this formulation, ΔW_{ext} is the virtual work of external loads applied on the system enclosed in the volume tube at a given time t. The two space-boundary terms (in brackets) model the effects of the material transport of the Lagrangian density, and of the virtual work of kinetic wrench, across the boundaries of the non-material tube. In the following subsections, each contribution of (56) are detailed. At the end, they will be introduced in the balance (56) to provide the weak and the strong form of the sliding rod dynamics.

4.4. External forces contribution

As regards, the virtual work of external forces, we simply need to reexpress its material expression (12), here restricted to $[\underline{X}, l]$, in terms of the non-material variable s:

$$\Delta W_{ext} = \int_0^d \Delta\zeta^T \bar{F}_{ext}\, ds + \Delta\zeta^T(0) F_{ext}^- + \Delta\zeta^T(d) F_{ext}^+, \tag{57}$$

where $\bar{F}_{ext}$ and F_{ext}^-, F_{ext}^+ here stand for a density of wrench per unit of s length and two concentrated wrenches in $s = 0$ and d. At the root, F_{ext}^- is such that $\mathbb{E}_1^T F_{ext}^- = C_{ext,1}^- \in \mathbb{R}$, and $\mathbb{E}_4^T F_{ext}^- = N_{ext,1}^- \in \mathbb{R}$, define the rolling torque and

[1] Note that, here and the following, these conventions should be used to distinguish g, η, $\xi = (K^T, \Gamma^T)^T$ and N as a function of s or X too. However, for the sake of concision, these fields are noted with the same notations regardless of this independency, the context removing the ambiguity.

the push-pull force, both applied on the rod through the sliding-pivot joint respectively. In the same expression, $\Delta\zeta$ is any compatible virtual displacement which satisfies (46) on $]0, d]$, while at $s = 0$, the compatibility with geometric BCs of the sliding-pivot joint imposes:

$$\Delta\zeta(0) = \delta\zeta(0) + \delta d\xi(0) = \delta\zeta_1(0)\mathbb{E}_1 + \delta d\xi(0). \tag{58}$$

which means that the rod can only be rotated at its root, with any virtual axial rotation $\delta\zeta_1(0) \in \mathbb{R}$, and push/pulled with δd along $\xi(0)$. Introducing such a compatible virtual displacement field into (57), allows the virtual work of external force to be rewritten as:

$$\Delta W_{ext} = \int_0^d (\delta\zeta + \xi\delta d)^T \bar{F}_{ext}\, ds + (\delta\zeta_1(0)\mathbb{E}_1 + \xi(0)\delta d)^T F^-_{ext} + (\delta\zeta(d) + \xi(d)\delta d)^T F^+_{ext}, \tag{59}$$

which can be recast as:

$$\Delta W_{ext} = \int_0^d \delta\zeta^T \bar{F}_{ext}\, ds + \delta\zeta_1(0) C^-_{ext,1} + \delta\zeta(d)^T F^+_{ext} + \delta d P_{ext}, \tag{60}$$

where P_{ext} is the generalized force associated with the generalized coordinate d, which reads as:

$$P_{ext} = \int_0^d \xi^T \bar{F}_{ext}\, ds + \xi^T(0) F^-_{ext} + \xi^T(d) F^+_{ext} = \int_0^d \xi^T \bar{F}_{ext}\, ds + K^T(0) C^-_{ext} + N^-_{ext,1} + \xi^T(d) F^+_{ext},$$

where note that the sliding kinematics makes appear the full external torque C^-_{ext} (including the reaction components exerted by the wall). Owing to action-reaction principle, C^-_{ext} can be detailed as $C^-_{ext} = (C^-_{ext,1}, -C_\perp(0)^T)^T$, with $C_\perp(0)^T = (C_2, C_3)(0)$, and we have finally:

$$P_{ext} = \int_0^d \xi^T \bar{F}_{ext}\, ds - K^T_\perp(0) C_\perp(0) + K_1(0) C^-_{ext,1} + N^-_{ext,1} + \xi^T(d) F^+_{ext}, \tag{61}$$

where we introduced the notation $K_\perp = (K_2, K_3)^T$.

4.5. Flux boundary contribution

Using the expression (46) of any compatible $\Delta\zeta$, in which $\delta\zeta$ and δd stand for two independent virtual displacements, allows the flux boundary terms of (56) to be rewritten as:

$$\left[\Delta\zeta^T \left(\frac{\partial \mathfrak{Q}}{\partial \eta}\right) \dot{d} - \mathfrak{Q}\delta d\right]_0^d = \left[\delta\zeta^T \left(\frac{\partial \mathfrak{Q}}{\partial \eta}\right)\right]_0^d \dot{d} + \left[\xi^T \left(\frac{\partial \mathfrak{Q}}{\partial \eta}\right) \dot{d} - \mathfrak{Q}\right]_0^d \delta d, \tag{62}$$

where we take $\delta\zeta(0) = \delta\zeta_1(0)\mathbb{E}_1$, to ensure its compatibility with the sliding-pivot joint at the root (see (58)).

4.6. Integral contribution

Using standard derivation rules, we are led to:

$$\int_0^d \delta\mathfrak{Q}\, ds = \int_0^d \left(\delta\eta^T \left(\frac{\partial \mathfrak{Q}}{\partial \eta}\right) + \delta\xi^T \left(\frac{\partial \mathfrak{Q}}{\partial \xi}\right) + \delta\dot{d} \left(\frac{\partial \mathfrak{Q}}{\partial \dot{d}}\right) + \delta N^T \left(\frac{\partial \mathfrak{Q}}{\partial N}\right)\right) ds. \tag{63}$$

Therefore, we recover the usual context of a closed inextensible Kirchhoff rod, where the material label X is replaced by the label s of the tube cross-sections. In particular, the variation δ being applied to $g(.)$ while t and s are maintained fixed, i.e. with $\delta t = \delta s = 0$, one can resort to the usual commutation relations (13), but now in terms of the base variables (t, s) (see Appendix A):

$$\delta\eta = \partial_t \delta\zeta + ad_\eta \delta\zeta \;\;,\;\; \delta\xi = \partial_s \delta\zeta + ad_\xi \delta\zeta\,. \tag{64}$$

Moreover, d being an ordinary variable in the vector space $\mathbb{R}$, we have the trivial commutation relation $\delta(d(d)/dt) = d(\delta d)/dt$. Inserting these commutation relations in (63), usual by part integration in space and time, and fixed time-end conditions, allow the integral contribution to be rewritten as:

$$\int_0^d \delta\mathfrak{L}\, ds = \int_0^d \delta\zeta^T \left(-\frac{\partial}{\partial t}\left(\frac{\partial \mathfrak{L}}{\partial \eta}\right) + ad_\eta^T\left(\frac{\partial \mathfrak{L}}{\partial \eta}\right) - \frac{\partial}{\partial s}\left(\frac{\partial \mathfrak{L}}{\partial \xi}\right) + ad_\xi^T\left(\frac{\partial \mathfrak{L}}{\partial \xi}\right)\right) + \delta N^T\left(\frac{\partial \mathfrak{L}}{\partial N}\right) ds$$
$$+ \left[\delta\zeta^T\left(\frac{\partial \mathfrak{L}}{\partial \xi} - \left(\frac{\partial \mathfrak{L}}{\partial \eta}\right)\dot{d}\right)\right]_0^d - \delta d\left(\int_0^d \frac{\partial}{\partial t}\left(\frac{\partial \mathfrak{L}}{\partial \dot{d}}\right) ds\right), \tag{65}$$

where from (58), $\delta\zeta(0) = \delta\zeta_1(0)\mathbb{E}_1$ in order to be compatible with the sliding-pivot joint at the root.

5. Non-material Cosserat-Poincaré formulation of a sliding rod

Inserting (60), (62) and (65) into (56), provides the weak-form of virtual works, which holds for any $\delta N(.)$, and any $(\delta\zeta(.), \delta d)$ compatible with the geometric constraints. Symbolically, we shall write:

$$\int_0^d \left(\delta\zeta^T I_1 + \delta N^T I_2\right) ds + \left[\delta\zeta^T I_3\right]_0^d + \delta d\,(I_4) = 0. \tag{66}$$

In the above expression "$I_1 = 0$" stands for the PDE for $g(.)$, i.e. the Cosserat-Poincaré equation of the non-material tube pause field over $]0, d[$:

$$\frac{\partial}{\partial t}\left(\frac{\partial \mathfrak{L}}{\partial \eta}\right) - ad_\eta^T\left(\frac{\partial \mathfrak{L}}{\partial \eta}\right) + \frac{\partial}{\partial s}\left(\frac{\partial \mathfrak{L}}{\partial \xi}\right) - ad_\xi^T\left(\frac{\partial \mathfrak{L}}{\partial \xi}\right) = \bar{F}_{ext}, \tag{67}$$

with boundary conditions imposed by the geometric constraint imposed at the rod's root in the wall:

$$r(0) = 0 \ , \ R(0)E_1 = e_1 \ , \tag{68}$$

as well as the BCs on forces, provided by the conditions "$I_3(0) = 0$" and "$I_3(d) = 0$" of (66):

$$\mathbb{E}_1^T\left(\frac{\partial \mathfrak{L}}{\partial \xi} - \left(\frac{\partial \mathfrak{L}}{\partial \eta}\right)\dot{d}\right)(0) = C_{ext,1}^- \ , \ \left(\frac{\partial \mathfrak{L}}{\partial \xi} - \left(\frac{\partial \mathfrak{L}}{\partial \eta}\right)\dot{d}\right)(d) = -F_{ext}^+. \tag{69}$$

As in the material case, these PDEs need to be supplemented with the reconstruction equation:

$$\partial_t g = g\hat{\eta}. \tag{70}$$

While (67) have the general form of Poincaré equations of Cosserat rods with s replacing X, it is in fact possible to set them in an alternative form more specific to sliding rods. To that end, let us first remark that in (55), $\mathfrak{L}$ can be detailed as $\mathfrak{L}(\eta_{_D}, \xi, N) = \mathfrak{T}(\eta_{_D}) - \mathfrak{U}(\xi, N)$ with $\mathfrak{T}$ and $\mathfrak{U}$ the densities of kinetic and strain energy respectively. Second, using the relations:

$$\frac{\partial \mathfrak{T}}{\partial \xi} = \left(\frac{\partial \mathfrak{T}}{\partial \eta_{_D}}\right)\left(\frac{\partial \eta_{_D}}{\partial \xi}\right) = \dot{d}\left(\frac{\partial \mathfrak{T}}{\partial \eta_{_D}}\right) \ , \ \frac{\partial \mathfrak{L}}{\partial \eta} = \frac{\partial \mathfrak{T}}{\partial \eta} = \frac{\partial \mathfrak{T}}{\partial \eta_{_D}}, \tag{71}$$

along with (42), (45) and the linearity of ad, it is straightforward to show that (67) takes the alternative form:

$$\frac{D}{Dt}\left(\frac{\partial \mathfrak{T}}{\partial \eta_{_D}}\right) - ad_{\eta_{_D}}^T\left(\frac{\partial \mathfrak{T}}{\partial \eta_{_D}}\right) - \frac{\partial}{\partial s}\left(\frac{\partial \mathfrak{U}}{\partial \xi}\right) + ad_\xi^T\left(\frac{\partial \mathfrak{U}}{\partial \xi}\right) = \bar{F}_{ext}, \tag{72}$$

with BCs:

$$r(0) = 0 \ , \ R(0)E_1 = e_1, \tag{73}$$

$$\mathbb{E}_1^T\left(\frac{\partial \mathfrak{U}}{\partial \xi}\right)(0) = -C_{ext,1}^- \ , \ \left(\frac{\partial \mathfrak{U}}{\partial \xi}\right)(d) = F_{ext}^+, \tag{74}$$

where the convective terms were removed from (69) by using (71). These equations which are equivalent to (67-69), can be interpreted as the non-material Poincaré equations of a sliding Cosserat rod (here rotated at its root). With our

rod kinematics, one needs to supplement them with the Kirchhoff Hookean constitutive law, along with the no-stretch nor shear condition provided by "$I_2 = 0$", i.e., with:

$$\frac{\partial \mathfrak{U}}{\partial K} = C = \mathcal{H}_a(K - \tilde{K}_o)\ ,\ \Gamma = E_1\ . \tag{75}$$

where in contrast to (29), all the fields are now s-dependent. These first dynamics which govern the time-evolution of $g(.)$, are here coupled with the ordinary differential equation (ODE) for the generalized coordinate d, which is symbolized by "$I_4 = 0$" in (66):

$$\int_0^d \frac{\partial}{\partial t}\left(\frac{\partial \mathfrak{L}}{\partial \dot{d}}\right) ds = \left[\mathfrak{L} - \dot{d}\left(\frac{\partial \mathfrak{L}}{\partial \dot{d}}\right)\right]_0^d + P_{ext}, \tag{76}$$

where note that we have the identities:

$$\left(\frac{\partial \mathfrak{L}}{\partial \dot{d}}\right) = \xi^T\left(\frac{\partial \mathfrak{T}}{\partial \eta_{_D}}\right) = \xi^T\left(\frac{\partial \mathfrak{T}}{\partial \eta}\right). \tag{77}$$

Moreover, using Reynolds transport theorem (51), allows this ODE to be rewritten as:

$$\frac{D}{Dt}\left(\frac{\partial L}{\partial \dot{d}}\right) = [\mathfrak{L}]_0^d + P_{ext}, \tag{78}$$

with $L = \int_0^d \mathfrak{L}\ ds$ the original Lagrangian of the deployed rod of Lagrangian density (55). Finally, the set of equations (72-76) with (61) provides a closed formulation of the dynamics of a sliding inextensible Kirchhoff rod as detailed in the next section.

Remark 6: Referring to section 2, the two operators $ad_{\eta_{_D}}$ and ad_ξ of (72), can be detailed as:

$$ad_{\eta_{_D}} = \begin{pmatrix} \hat{\Omega}_{_D} & 0 \\ \hat{V}_{_D} & \hat{\Omega}_{_D} \end{pmatrix},\ ad_\xi = \begin{pmatrix} \hat{K} & 0 \\ \hat{E}_1 & \hat{K} \end{pmatrix}, \tag{79}$$

where from (45), $\Omega_{_D} = \Omega + \dot{d}K$ and $V_{_D} = V + \dot{d}E_1$. Then, using (79), as well as the relation which holds for any $W \in \mathbb{R}^3$:

$$D_t(RW) = R(D_tW + \Omega_{_D} \times W), \tag{80}$$

in (72), gives:

$$\rho A D_t(v_{_D}) = \partial_s n + \bar{n}\ ,\ \rho I D_t(\omega_{_D}) + \omega_{_D} \times (\rho I \omega_{_D}) = \partial_s c + t_1 \times n + \bar{c}, \tag{81}$$

where we introduced the spatial vectors and tensors: $\omega_{_D} = R\Omega_{_D}$, $v_{_D} = RV_{_D}$, $c = RC$, $n = RN$, $\bar{n} = R\bar{N}$, $\bar{c} = R\bar{C}$, $t_1 = RE_1$ and $I = RJR^T = R\text{diag}(J_1, J_2, J_3)R^T$. Equations (81) are the non-material PDEs of an inextensible Kirchhoff rod in the inertial frame. Once restricted to the planar case, and with E_1 replaced by Γ, they take the form of the PDEs of a Reissner sliding rod in the Eulerian-Lagrangian approach, as they were first derived [13].

Remark 7: For verification purpose, one can get the same formulation by directly shifting the weak-form of virtual works from the Lagrangian to our hybrid setting, i.e. without resorting to the extended Hamilton principle. To this end, we reconsider the material weak form of virtual works (28), but applied to the truncated material domain $[\underline{X}, l]$, and in the form (B.2) of Appendix B:

$$\int_{\underline{X}}^{l} \delta\zeta^T\left(\frac{\partial}{\partial t}\left(\frac{\partial \mathfrak{T}}{\partial \eta}\right) - ad_\eta^T\left(\frac{\partial \mathfrak{T}}{\partial \eta}\right) - \bar{F}_{ext}\right) dX = -\int_{\underline{X}}^{l} \delta\mathfrak{U}\ dX + \delta\zeta(\underline{X})^T F_{ext}^- + \delta\zeta(l)^T F_{ext}^+, \tag{82}$$

where all the fields are Lagrangian, i.e. X-dependent, while F_{ext}^- and F_{ext}^+ denote the concentrated external wrenches applied to the $\underline{X}$ and l-material-cross-sections. This balance of virtual works must hold for any admissible field $\delta\zeta$, such that $\delta\zeta(\underline{X}) = \delta\zeta_1(\underline{X})\mathbb{E}_1 + \delta\zeta_4(\underline{X})\mathbb{E}_4$ since one considers a sliding pivot joint which can only transmit an external axial torque and push-pull force, at the root $X = \underline{X}$. Using the kinematic transformations of section 4.1, one can change all the X-dependent fields into their s-dependent counterparts, and transform (82) into:

$$\int_0^d \Delta\zeta^T\left(\frac{D}{Dt}\left(\frac{\partial \mathfrak{T}}{\partial \eta_{_D}}\right) - ad_{\eta_{_D}}^T\left(\frac{\partial \mathfrak{T}}{\partial \eta_{_D}}\right) - \bar{F}_{ext}\right) ds = -\int_0^d \Delta\mathfrak{U}\ ds + \Delta\zeta(0)^T F_{ext}^- + \Delta\zeta(d)^T F_{ext}^+, \tag{83}$$

where owing to (42), $\Delta\mathfrak{U} = \delta\mathfrak{U} + \delta d\partial_s\mathfrak{U}$, and $\Delta\zeta$ is any virtual displacement field compatible with the internal rod kinematics and the geometric BC of the sliding pivot joint at the root. Using the expressions (46) and (58) of such compatible fields in (83), provides us with (64) and by part integration with respect to s, the weak form for the dynamics of the field of pause $g(.) : s \in [0, d] \mapsto g(s) \in SE(3)$:

$$\int_0^d \delta\zeta^T \left(\frac{D}{Dt}\left(\frac{\partial\mathfrak{T}}{\partial\eta_D}\right) - ad^T_{\eta_D}\left(\frac{\partial\mathfrak{T}}{\partial\eta_D}\right) - \frac{\partial}{\partial s}\left(\frac{\partial\mathfrak{U}}{\partial\xi}\right) + ad^T_\xi\left(\frac{\partial\mathfrak{U}}{\partial\xi}\right) - \bar{F}_{ext}\right) ds$$

$$+ \int_0^d \delta N^T \left(\frac{\partial\mathfrak{U}}{\partial N}\right) ds = -\left[\delta\zeta^T(s)\left(\frac{\partial\mathfrak{U}}{\partial\xi}\right)(s)\right]_0^d + \delta\zeta_1(0)^T C^-_{ext,1} + \delta\zeta(d)^T F^+_{ext}, \tag{84}$$

which being true for any $(\delta\zeta(.), \delta\zeta_1(0), \delta N(.))$ considered as independent between them, allows recovering the closed dynamic formulation (72-74) for $g(.)$. The same expression of compatible virtual displacement field provides the weak form for d, which then takes the primary expression:

$$\delta d \int_0^d \xi^T \left(\frac{D}{Dt}\left(\frac{\partial\mathfrak{T}}{\partial\eta_D}\right) - ad^T_{\eta_D}\left(\frac{\partial\mathfrak{T}}{\partial\eta_D}\right) - \bar{F}_{ext}\right) ds = \delta d\left(K_1(0)C^-_{ext,1} - K^T_\perp(0)C_\perp(0) + N^-_{ext,1} + \xi(d)^T F^+_{ext} - [\mathfrak{U}]_0^d\right), \tag{85}$$

which holds for any δd. Now, tedious but straightforward calculations based on the kinematics of section 4.1 along with the identity (77), and the properties of the ad map, provide the key relation:

$$\int_0^d \xi^T \left(\frac{D}{Dt}\left(\frac{\partial\mathfrak{T}}{\partial\eta_D}\right) - ad^T_{\eta_D}\left(\frac{\partial\mathfrak{T}}{\partial\eta_D}\right)\right) ds = \int_0^d \frac{\partial}{\partial t}\left(\frac{\partial\mathfrak{L}}{\partial\dot{d}}\right) ds + \left[\left(\frac{\partial\mathfrak{L}}{\partial\dot{d}}\right)\dot{d} - \mathfrak{T}\right]_0^d. \tag{86}$$

Using this relation as well as (61), in (85), one can rewrite the weak form for d as:

$$\delta d \int_0^d \left(\frac{\partial}{\partial t}\left(\frac{\partial\mathfrak{L}}{\partial\dot{d}}\right)\right) ds - \delta d\,[\mathfrak{L}]_0^d + \delta d\left[\frac{\partial\mathfrak{L}}{\partial\dot{d}}\right]_0^d \dot{d} = \delta d P_{ext}. \tag{87}$$

Finally, this balance holding for any δd, one recovers the ODE for d (76), as it is provided by the extended Hamilton principle (56).

5.1. Closed dynamics of a sliding inextensible rod

To derive the detailed formulation of the dynamics of the rod, it suffices first to insert the Lagrangian density (54) into the Poincaré equation (67). This gives:

$$\mathcal{M}(\partial_t\eta + \xi\ddot{d} + \partial_t\xi\dot{d}) - ad^T_\eta\mathcal{M}(\eta + \xi\dot{d})$$

$$+\dot{d}\left(\mathcal{M}(\partial_s\eta + \dot{d}\partial_s\xi) - ad^T_\xi\mathcal{M}(\eta + \dot{d}\xi)\right) - \partial_s\Lambda + ad^T_\xi\Lambda = \bar{F}_{ext}, \tag{88}$$

where we introduced the field of internal stress wrench (31):

$$C = \mathcal{H}_a(K - \tilde{K}_o)\ ,\ N \text{ s.t. } \Gamma - E_1 = 0, \tag{89}$$

which defines the constitutive law of the rod. This PDE needs to be supplemented with the BCs:

$$r(0) = 0\ ,\ R(0)E_1 = e_1\ ,\ \mathbb{E}_1^T\Lambda(0) = -C^-_{ext,1}\ ,\ \Lambda(d) = F^+_{ext}. \tag{90}$$

Regarding the ODE of d (76), using (54,77) and (61), we get:

$$\int_0^d \partial_t\xi^T\mathcal{M}\eta + \xi^T\mathcal{M}(\partial_t\eta + \xi\ddot{d} + 2\partial_t\xi\dot{d})\,ds = \int_0^d \xi^T\bar{F}_{ext}\,ds + \xi^T(d)F^+_{ext}$$

$$+\frac{1}{2}\left[(\eta - \xi\dot{d})^T\mathcal{M}(\eta + \xi\dot{d}) - (K - \tilde{K}_o)^T\mathcal{H}_a(K - \tilde{K}_o)\right]_0^d - K^T_\perp(0)C_\perp(0) + K_1(0)C^-_{ext,1} + N^-_{ext,1}, \tag{91}$$

where let us remark that $\eta(0) = \eta_1(0)\mathbb{E}_1$ (the non-material tube cross section $s = 0$, can only rotate around the normal to the wall with the angular velocity $\eta_1(0)E_1$). Finally, once supplemented with a model of the external forces, (88-91) form a closed formulation of the sliding rod dynamics.

5.2. Special cases

We now instantiate the formulation (88-91) in several simple contexts.

Instance 1: A non sliding rod: When the sliding degree of freedom of the rod is locked, for instance by imposing $d = l$, we need to remove all the d-dependency in the above formulation. In this special case, the ODE (91) disappears, while (88) and (90) take the usual material form (36,37) of the dynamics of a rod connected to a fixed support through an actuated pivot joint, in which $X = s$.

Instance 2: A rigid sliding rod: Another special simple case, consists in freezing the field $s \mapsto \xi(s)$ with respect to time, and to push/pull such a rigid rod in, or outside the wall with an axial external force $F^-_{ext} = N^-_{ext,1}\mathbb{E}_4$ based at its root. If furthermore, this sliding rigid rod remains straight while moving, one has $\xi = \mathbb{E}_4, \forall s \in [0, d]$. In this reciprocal case to the previous one, only the ODE (91) survives and takes the trivial form:

$$\int_0^d (\xi^T \mathcal{M} \xi)\ddot{d}\, ds = \left(\int_0^d \rho A ds\right)\ddot{d} = \frac{1}{2}\rho A \dot{d}^2 - \frac{1}{2}\rho A \dot{d}^2 + N^-_{ext,1}, \tag{92}$$

where we used $\xi^T \mathcal{M} \xi = \rho A$ as well as the fact that $\eta = 0$, since coming back to (45), the rigid rod can only have a sliding velocity component. Finally, defining the time varying mass of this sliding rigid rod:

$$m = \int_0^d \rho A ds = \rho A d, \tag{93}$$

the ODE (92) then matches with the balance of kinetic momentum, which in this simple case, takes the Newtonian form[2]:

$$m\ddot{d} = N^-_{ext,1}, \tag{94}$$

where remind that m is here d-dependent. Going further, including the inner piece of beam in the formulation, one recovers the standard Newton law (94) but with $m = \rho A l$, the constant mass of the entire rod considered as a closed system, and $N^-_{ext,1}$ now denoting the external push-pull force applied to the material cross-section $X = 0$, which coincides with $s = d - l$.

Instance 3: A slowly sliding rod: Another case which is of special interest, consists of the quasi-steady regime in which d slowly evolves while the influence of its time-derivatives on the dynamics can be neglected. In this case, the g-dynamics are those of the classical material setting (36-39) where the space domain $[0, d(t)]$ needs to be updated at each time. This is the usual regime used for modelling growing plants [31] or concentric tubes robots [32]. As regards the ODE for d, it is reduced to:

$$\int_0^d \frac{\partial \xi}{\partial t}^T \mathcal{M}\eta + \xi^T \mathcal{M}\frac{\partial \eta}{\partial t} ds = \int_0^d \frac{\partial}{\partial t}\left(\xi^T \mathcal{M}\eta\right) ds = \frac{d}{dt}\int_0^d \xi^T \mathcal{M}\eta\, ds = P_{ext}, \tag{95}$$

where the flux component is neglected.

Instance 4: A rod subjected to an imposed sliding and rotating motion: Most of the models proposed so far for studying sliding rods, assume that the sliding motion is imposed. This restricted context can be deduced from the above model, by removing the ODE (91), and integrating the PDE (88) in which $d, \dot{d}$ and $\ddot{d}$ are replaced by some prescribed time laws $t \mapsto (d(t), \dot{d}(t), \ddot{d}(t))$. Similarly, imposing the time-evolution of the rolling angle θ at the root, leads to replace the two rotational BCs of (90), by the unique one : $R(0) = \exp(\theta(t)\hat{E}_1)$.

[2]When the rod deploys outside the wall, it can be considered as an open system that accretes new cross-sections at its root with a zero relative velocity. In this case, this is known after Mescerskii [30] that the kinetic momentum balance takes the Newton form (94). When the rod retracts inside the wall, the same picture holds, but the cross sections can be seen as detaching from the rod at the root.

6. Extension to the inner part of the sliding rod

The above model can be extended to include the part of the rod inside the wall (cf. figure 2) as this is done for the extended sliding spaghetti problem in [17]. To that end, one needs to reapply the same approach but to the left part of the rod considered as an open system enclosed in a second non-material tube that is parameterized with s now running from $d-l$ to 0. This further non-material domain is denoted $\mathcal{D}^\star = [d-l, 0]$, and all the variables related to it (tensor fields, vectors...), are distinguished from their counterparts on $\mathcal{D} = [0, d]$, with a "$\star$". Mechanically, the tubular guide across which this other piece of rod slides, prevents it from moving laterally. Thus, one can describe its motion as that of an inextensible rod subjected to a translation along, and a rotation around its material axis only. In these restricted conditions, the full three-dimensional $g(.)$ of the above context, is changed into $g^\star(.) = (R^\star, x^\star e_1)(.)$ with $R^\star(.) = \exp(\theta^\star(.)\hat{E}_1)$, and $x^\star(.)e_1$ the positional field of the tube cross-sections in (o, e_1, e_2, e_3). The rod being inextensible, the configuration of the inner piece is defined by all the possible $(\theta^\star(.), d)$, where $\theta^\star(.)$ stands for a rolling angle field along its axis, and d is the sliding translation of the previous context. In $s = 0$, this piece of twistable rod is smoothly connected to the outer inextensible Kirchhoff rod. Moreover, the inner piece being free to roll and translate along the guide, the internal torsion couple and axial tension force of the two pieces, are continuous across the junction $s = 0$. Applying the very same extended Hamilton's principle to the non-material domain $\mathcal{D}^\star$ as we did for $\mathcal{D}$, leads to a PDE for $\theta^\star(.)$, and a second ODE for d.

The PDE for $\theta^\star(.)$ is given by applying (72-74) to $\mathcal{D}^\star$, which gives after some algebra:

$$\forall s \in]d-l, 0[\ , \rho J_1 D_t(D_t\theta^\star) - \partial_s C_1^\star = 0, \tag{96}$$

with the constitutive law and inextensibility condition on $[d-l, 0]$:

$$C_1^\star = GJ_1K_1^\star = GJ_1\partial_s\theta^\star \ \ , \ \partial_s x^\star = 1, \tag{97}$$

and the boundary and continuity conditions of the twist torque field at the junction $s = 0$:

$$C_1^\star(d-l) = -C_{ext,1}^{\star -}\ , C_1^\star(0) = C_1(0) = \mathbb{E}_1^T\Lambda(0), \tag{98}$$

where $C_{ext,1}^{\star -}$ now defines the prescribed axial torque exerted on the material cross-section $X = 0$. Note that this PDE is the exact counterpart for $\mathcal{D}^\star$, of (88-90) for $\mathcal{D}$.

Similarly, the application of the extended Hamilton's principle to the non-material volume inside the wall provides an ODE for d similar to (76), but with $[0, d]$ replaced by $[d-l, 0]$. After some straightforward algebra, we are led to:

$$\rho A(l-d)\ddot{d} = (\partial_s\theta^\star)(d-l)C_{ext,1}^{\star -} + N_{ext,1}^{\star -} + (\partial_s\theta^\star)(0)C_1(0) + N_1(0), \tag{99}$$

where $N_{ext,1}^{\star -}$ stands for the prescribed axial force exerted on the material cross-section $X = 0$. Note that this ODE is the counterpart of (91), for the non-material volume inside the wall.

Remark 8: A closed formulation of the extended sliding rod is provided by gathering the PDEs (88-90) and (96,97), with one of the two ODEs for d, namely (91) or (99). Remarkably, while the first of these two ODEs makes appear complex transported terms coming from extended Hamilton's principle, the second is much more simple and intuitive. In the numerical illustration reported later, we will use these two ODEs to check whether they are equivalent. Beyond the emblematic example here addressed, for any rod that axially flows through a sequence of non-material sub-domains, while one has to consider PDEs for each of them, the inextensibility condition offers a freedom for the modeler, since one can chose one of its ODEs[3] (the simplest), to close the dynamic formulation.

[3] All of them being compatible thanks to action-reaction principle.

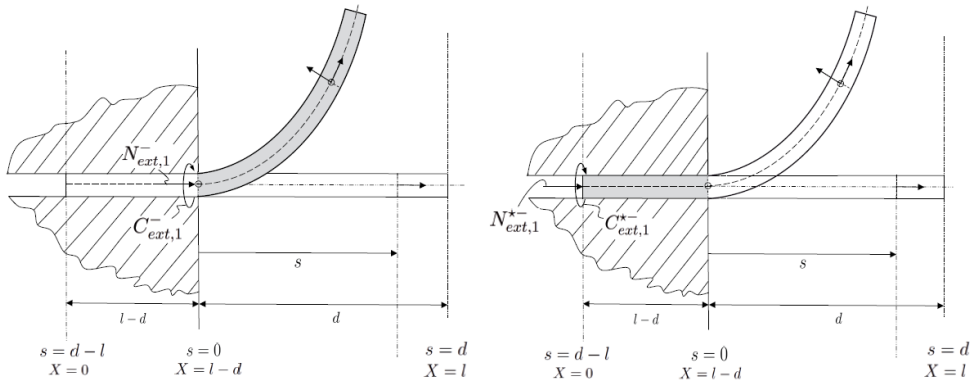

Figure 2. Non-material domains $\mathcal{D} = [0, d]$ and $\mathcal{D}^\star = [d - l, 0]$ for the study of the extended sliding rod.

7. Numerical implementation

To numerically exploit the above formulation, one could use the GE-FEM applied to the weak form of virtual work (66). Here, we use another approach recently proposed in [27]. The approach is based on a parametrization of the configuration of the rod in terms of its strains which are then reduced on a Ritz basis of polynomials. Note that although it resembles the assumed modes method of flexible multibody system dynamics, it differs from it by the fact that the Ritz reduction is applied to strain fields. Then, spatially integrating these strain fields, allows the fields of absolute transformations $g(.)$ to be reconstructed in a geometrically exact manner. As a result, the approach works in finite transformations. In [27], it is shown that this strain-based parametrization allows to recover the results of the GE-FEM in the pure material case of non-sliding rods. In the present context, we extend it to our hybrid (Eulerian/Lagrangian) setting, by applying it to our sliding rod. For the sake of concision, in all the subsequent developments, we shall denote $\partial./\partial t$ and $\partial./\partial s$ by a dot and a prime respectively. Moreover, the external axial force $N^-_{ext,1}$, and the rolling external torque $C^-_{ext,1}$, if defined as some imposed functions of time, are denoted $N^-_{ext,1}(t)$ and $C^-_{ext,1}(t)$ respectively.

7.1. Simulation algorithm

We now shift from the definition (40) of the configuration space of the piece of rod out of the wall, to another, based on the strain parametrization of [27]. In this case, the configurations of this piece are defined by the set of $(\theta, d, \xi(.))$s, where θ denotes the rolling angle of the root (non-material) cross section $s = 0$, while the strain field $\xi(.)$ is reduced on a basis of n Ritz functions gathered in a $3 \times n$ matrix Φ :

$$\xi(s) - \tilde{\xi}_o(s) = \begin{pmatrix} K(s) \\ E_1 \end{pmatrix} - \begin{pmatrix} \tilde{K}_o(s) \\ E_1 \end{pmatrix} = \begin{pmatrix} \Phi(s) q_\epsilon \\ 0_{3\times 1} \end{pmatrix}, \tag{100}$$

where we remind that $\xi_o(.) = (K_o^T, E_1^T)^T(.)$ is known, while the index ϵ refers to the strain measurement $\epsilon = \xi - \tilde{\xi}_o$. In these numerical conditions, the configuration space (40) is changed into the finite dimensional space of all possible $(\theta, d, q_\epsilon^T)^T$. The use of this second definition of the configuration space is attested by the fact that for any $(\theta, d, q_\epsilon^T)^T$, one can reconstruct the cross-sectional pause field of the rod $g(.)$ at any time-step of a global simulation time-loop, by space-integrating the following ODE from $s = 0$ to d:

$$g' = g\hat{\xi}, \tag{101}$$

with ξ defined by (100), and initial conditions:

$$g(0) = \text{diag}(\exp(\theta\hat{E}_1), 1). \tag{102}$$

On this reduced definition of the configuration space, the dynamics of the rotating sliding rod take the usual matrix form:

$$\begin{pmatrix} Q_\theta(t) \\ Q_d(t) \\ 0_{n\times 1} \end{pmatrix} = \begin{pmatrix} M_{\theta\theta} & M_{\theta d} & M_{\theta\epsilon} \\ M_{d\theta} & M_{dd} & M_{d\epsilon} \\ M_{\epsilon d} & M_{\epsilon\theta} & M_{\epsilon\epsilon} \end{pmatrix} \begin{pmatrix} \ddot{\theta} \\ \ddot{d} \\ \ddot{q}_\epsilon \end{pmatrix} + \begin{pmatrix} Q_{v,\theta} \\ Q_{v,d} \\ Q_{v,\epsilon} \end{pmatrix} + \begin{pmatrix} Q_{c,\theta} \\ Q_{c,d} \\ Q_{c,\epsilon} \end{pmatrix} + \begin{pmatrix} 0 \\ 0 \\ K_{\epsilon\epsilon} q_\epsilon \end{pmatrix}, \tag{103}$$

where from left to right, we find the vector of imposed generalized forces with $Q_\theta(t) = \mathbb{E}_1^T F_{ext}^-(t) = C_{ext,1}^-(t)$ and $Q_d(t) = \mathbb{E}_4^T F_{ext}^-(t) = N_{ext,1}^-(t)$, the (symmetric) matrix of generalized inertia, the vector of generalized accelerations and those of velocity and configuration dependent forces. The restoring forces being linear, we introduced the generalized stiffness matrix of the rod:

$$K_{\epsilon\epsilon} = \int_0^d \Phi^T \mathcal{H}_a \Phi \, ds, \tag{104}$$

which being constant, can be calculated once for all, outside the simulation time-loop. Then, one can consider the system having the same inertia but fully actuated. The model of such a system is given by (103) in which the restoring forces are replaced by a vector of generalized internal forces, noted $Q_{a,\epsilon}$. The dynamics of this other system take the form:

$$\begin{pmatrix} Q_{a,\theta} \\ Q_{a,d} \\ Q_{a,\epsilon} \end{pmatrix} = \begin{pmatrix} M_{\theta\theta} & M_{\theta d} & M_{\theta\epsilon} \\ M_{d\theta} & M_{dd} & M_{d\epsilon} \\ M_{\epsilon\theta} & M_{\epsilon d} & M_{\epsilon\epsilon} \end{pmatrix} \begin{pmatrix} \ddot{\theta} \\ \ddot{d} \\ \ddot{q}_\epsilon \end{pmatrix} + \begin{pmatrix} Q_{v,\theta} \\ Q_{v,d} \\ Q_{v,\epsilon} \end{pmatrix} + \begin{pmatrix} Q_{c,\theta} \\ Q_{c,d} \\ Q_{c,\epsilon} \end{pmatrix} \tag{105}$$

where $Q_{a,\theta}$, $Q_{a,d}$ and $Q_{a,\epsilon}$ now define some fictitious generalized actuation forces while the other components are the same as in (103). For any state $(\theta, \dot{\theta}, d, \dot{d}, q_\epsilon^T, \dot{q}_\epsilon^T)^T$, the above model is an inverse dynamic model with inputs $\ddot{\theta}$, $\ddot{d}$, $\ddot{q}_\epsilon$, and outputs $Q_{a,\theta}$, $Q_{a,d}$ and $Q_{a,\epsilon}$. Using the more concise notations $q = (\theta, d, q_\epsilon^T)^T$ and $Q_a^T = (Q_{a,\theta}, Q_{a,d}, Q_{a,\epsilon}^T)^T$, the model (105) can be equivalently realized by an algorithm that we formally note [27]:

$$Q_a = IDM(q, \dot{q}, \ddot{q}), \tag{106}$$

where IDM here means "Inverse Dynamic Model". This algorithm computes the outputs Q_a from the inputs $\ddot{q}$ for any state $x = (q^T, \dot{q}^T)^T$. Applied at each fixed time of the simulation, it consists of the s-integration in cascade of two ODEs with respect to s. The first is a forward integration (from the root $s = 0$ to the tip $s = d$) that computes the fields $(g, \eta, \dot{\eta})$ along the rod from the knowledge of the state variables and inputs $(q, \dot{q}, \ddot{q})$. Time-differentiating (101) twice, provides this first model, which reads:

$$g' = g\hat{\xi} \ , \ \eta' = -ad_\xi \eta + \dot{\xi} \ , \ \dot{\eta}' = -ad_\xi \dot{\eta} - ad_{\dot{\xi}} \eta + \ddot{\xi}, \tag{107}$$

in which one has to introduce (100), and which needs to be integrated from $s = 0$, with initial conditions:

$$g(0) = \text{diag}(\exp(\theta\hat{E}_1), 1) \ , \ \eta(0) = \dot{\theta}\mathbb{E}_1 \ , \ \dot{\eta}(0) = \ddot{\theta}\mathbb{E}_1. \tag{108}$$

Once all the kinematic fields $(g, \eta, \dot{\eta})$ are known, one can go to the second step of the cascade integration. Since the time is fixed, one can use the PDE (88) as a spatial ODE for $\Lambda = (C^T, N^T)^T$ that we integrate backward, i.e. from $s = d$, where the external force is known, to the root $s = 0$. Referring to (88), this second ODE reads:

$$\Lambda' = ad_\xi^T \Lambda + \mathcal{M}(\dot{\eta} + \xi\ddot{d} + \dot{\xi}\dot{d}) - ad_\eta^T \mathcal{M}(\eta + \xi\dot{d}) + \dot{d}(\mathcal{M}(\eta' + \dot{d}\xi') - ad_\xi^T \mathcal{M}(\eta + \dot{d}\xi)) - \bar{F}_{ext}, \tag{109}$$

and, needs to be integrated from $s = d$, with initial conditions:

$$\Lambda(d) = F_{ext}^+, \tag{110}$$

where we used the BCs of (90). Finally, once these two sets of ODEs integrated, the algorithm feeds back two of the expected outputs:

$$Q_{a,\theta} = C_{ext,1}^- = -\mathbb{E}_1^T \Lambda(0) \ , \ Q_{a,\epsilon} = -\int_0^d \Phi^T C \, ds. \tag{111}$$

It remains to compute the third output $Q_{a,d}$. To that end, note that the ODE (91) provides the expression of $Q_{a,d} = N^-_{ext,1}$ as:

$$Q_{a,d} = \int_0^d \left(\dot{\xi}^T \mathcal{M}\eta + \xi^T \mathcal{M}(\dot{\eta} + \xi\ddot{d} + 2\dot{\xi}\dot{d}) \; - \xi^T \bar{F}_{ext}\right) ds - \xi^T(d) F_{ext}(d) +$$
$$+ \tfrac{1}{2}\left[(K - \tilde{K}_o)^T \mathcal{H}_a (K - \tilde{K}_o) - (\eta - \xi\dot{d})^T \mathcal{M}(\eta + \xi\dot{d})\right]_0^d - K_\perp^T(0) C_\perp(0) + K_1(0) C^-_{ext,1}. \tag{112}$$

Therefore, defining a s-field $Q_{a,d}(.)$, one can backward integrate the further ODE:

$$Q'_{a,d} = \xi^T \bar{F}_{ext} - \dot{\xi}^T \mathcal{M}\eta - \xi^T \mathcal{M}(\dot{\eta} + \xi\ddot{d} + 2\dot{\xi}\dot{d}), \tag{113}$$

with initial condition:

$$Q_{a,d}(d) = \frac{1}{2}\left[(K - \tilde{K}_o)^T \mathcal{H}_a (K - \tilde{K}_o) - (\eta - \xi\dot{d})^T \mathcal{M}(\eta + \xi\dot{d})\right](d) - \xi^T(d) F^+_{ext}, \tag{114}$$

and use the final value of this backward integration to get the last expected output of the algorithm:

$$Q_{a,d} = Q_{a,d}(0) - \frac{1}{2}\left[(K - \tilde{K}_o)^T \mathcal{H}_a (K - \tilde{K}_o) - (\eta - \xi\dot{d})^T \mathcal{M}(\eta + \xi\dot{d})\right](0) + K_\perp^T(0) C_\perp(0) - K_1(0) C^-_{ext,1},$$

with $\eta(0) = \dot{\theta}\mathbb{E}_1$. Note that the two backward ODEs (109) and (113), can be gathered with $Q'_{a,\epsilon} = -\Phi^T C$ of (111) in a single one for $(\Lambda, Q_{a,\epsilon}, Q_{a,d})$. Finally, it is worth noting that the above sets of ODEs are integrated at each time step, along a domain of variable length d.

Using the identity of (105) and (106), it becomes straightforward to calculate at each time of a simulation, the residual vector r_{es} of the dynamic balance (103) with this IDM. In effect, one has:

$$r_{\text{es}}(q, \dot{q}, \ddot{q}, t) = IDM(q, \dot{q}, \ddot{q}) + (0, 0, (K_{\epsilon\epsilon} q_\epsilon)^T)^T - Q(t), \tag{115}$$

where $Q(t) = (Q_\theta(t), Q_d(t), 0_{1\times n})^T$ stands for the vector of actual (not fictitious), imposed external forces. To numerically integrate the dynamics, we used a one-step implicit time integrator of the Newmark class. This time-integrator scheme requires the linearized dynamics of (103) to be calculated. This can be easily achieved by using the tangent linearized algorithm, noted $TIDM$, to the IDM. This further algorithm is an input-output map of the generic form:

$$\Delta Q_a = TIDM(q, \dot{q}, \ddot{q}, t, \Delta q, \Delta\dot{q}, \Delta\ddot{q}). \tag{116}$$

It is deduced from the IDM by perturbing its inputs whose effects are propagated linearly up to its outputs. Finally, introducing in these two algorithms the constraints imposed by the implicit scheme on $(q, \dot{q}, \ddot{q})$ and their increments $(\Delta q, \Delta\dot{q}, \Delta\ddot{q})$, provides a natural way to calculate the residual vector (115) and its Jacobian (tangent stiffness) under constraint of the integration scheme. These residual vector and its Jacobian are then used in a Newton-loop, to correct at each step of time, the rod state, starting from an initial guess, up to nullify the residual vector (115), and to increment time.

Remark 9: In the wake of section 6 and remark 8, one can easily adapt the above numerical resolution to the dynamics of the full rod consisting of its internal and external pieces. In this wider context, the reduced inverse Lagrangian model of the entire rod also takes the form of (103), in which q_ϵ now contains some further strain coordinates which parameterize the twist field $K_1^\star(.)$ of the internal piece, on an additional Ritz basis $\Phi^\star$. Moreover, θ then defines the rolling angle of the cross section $X = 0$, while the vector of external forces $(Q_d, Q_\theta, 0_{1\times n})^T(t)$ is replaced by that of axial forces and rolling torques applied to this section and noted in this context $(Q_d^\star, Q_\theta^\star, 0_{1\times n})^T(t)$. An extended IDM algorithm allows calculating all the matrices of this full model. As in the previous case, this further IDM starts with a forward ODE on kinematics which is now piecewise integrated from $s = d - l$ to $s = d$, and continues with a piecewise backward ODE on internal stress from $s = d$ to $s = d - l$. In details, one starts with the forward integration of $\theta^{\star\prime} = K_1^\star$ and its time-differentials, whose final conditions at $s = 0$ feed the initial ones of (107). Similarly, the backward ODE on internal stress consists of the backward integration of stress balance (109), whose final condition at $s = 0$, feeds the

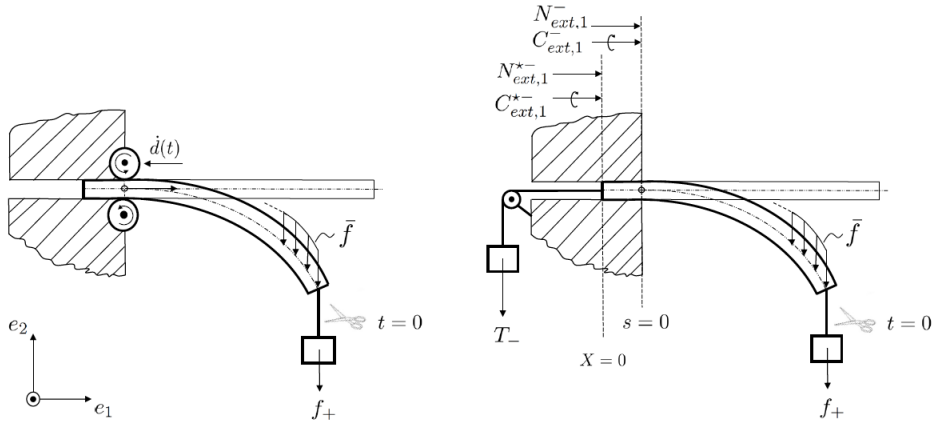

Figure 3. Conditions of the examples reported below. In all cases, the outer part of the rod is subjected to a uniform density of vertical external forces $\bar{f}$ and a tip concentrated force f_+. In example 1, the sliding motion is imposed at the root (e.g. by two wheels rolling without slipping along the rod as schematized on the left). In example 2 one exerts on the inner piece of the rod, a second force (T_-) as represented on the right. In both cases, at time $t = 0$, the left tip force f_+ is instantaneously removed (e.g. by cutting a link between the rod and an attached mass to it). For other examples (3 and 4), we impose more general loads through arbitrary push-pull forces and rolling torques applied on $X = 0$ ($N^{\star-}_{ext,1}, C^{\star-}_{ext,1}$), or at the root in the wall $s = 0$ ($N^-_{ext,1}, C^-_{ext,1}$) (see right schematic).

initial condition of the backward integration of (96). At the end, this extended algorithm feeds back the internal stress fields along the entire rod, i.e. $\Lambda(.)$ and $C^\star_1(.)$. It then computes $Q^\star_{a,\theta} = C^{\star-}_{ext,1} = -C^\star_1(d-l)$, while $Q^\star_{a,\epsilon}$ is computed by projecting these stress fields onto the Ritz basis of the two pieces of rod.

Finally, the ODE (99) provides $Q^\star_{a,d} = N^{\star-}_{ext,1}$ according to:

$$Q^\star_{a,d} = \rho A(l-d)\ddot{d} + Q_{a,d} + (\partial_s\theta^\star)(0)Q_{a,\theta} - (\partial_s\theta^\star)(d-l)Q^\star_{a,\theta}, \tag{117}$$

where $Q_{a,d} = N^-_{ext,1} = -N_1(0)$ and $Q_{a,\theta} = C^-_{ext,1} = -C_1(0)$, are directly given by the final conditions of the backward integration of (109). Perturbing the inputs of this extended IDM provides an extended $TIDM$ useful for calculating the tangent stiffness operator to the full rod dynamics.

7.2. Illustrative examples

In the following, this algorithm is applied to four examples. The first consists in imposing a prescribed retrieving motion to a sliding beam initially deployed and deformed in a plane (2D), and to integrate the forward dynamics of the rod pause fields $g(.)$, while solving the inverse dynamics for d. In the second example, the same rod is pulled by applying a constant axial force at its material root $X = 0$, while its forward dynamics are solved. In the third example, a rod is pulled and rotated in the three-dimensions (3D) by a pulling force and a rolling torque both applied at the orifice in the wall $s = 0$. Example 4 deals with the deployment of a pre-curved rod, i.e. we address the full three-dimensional forward dynamics of an un-twistable pre-curved rod subjected to a push-pull force at $X = 0$. Like in the model previously derived, in all the examples, the inertial frame (o, e_1, e_2, e_3) is positioned at the orifice of the guide in the wall, with e_1, the unit normal to the wall. The simulation of example 4 is carried out with a fixed Newmark time-step $\Delta t = 0.1$s, while for examples 1 to 3, Δt is refined from 0.1s to 0.001s, in order to adapt integration to the increasing frequency of the oscillations. The duration of simulations is 10s for example 4, and 5.5s for all others.

7.2.1. Example 1: "The sliding spaghetti problem": 2D retrieval of a sliding rod by imposing a sliding motion $t \mapsto d(t)$

We here consider a planar test proposed in [16]. The conditions of the test are those indicated in figure 3(a). A rectangular cross-sectional rod of length $l = 5$m is considered first as entirely deployed out of a wall and statically

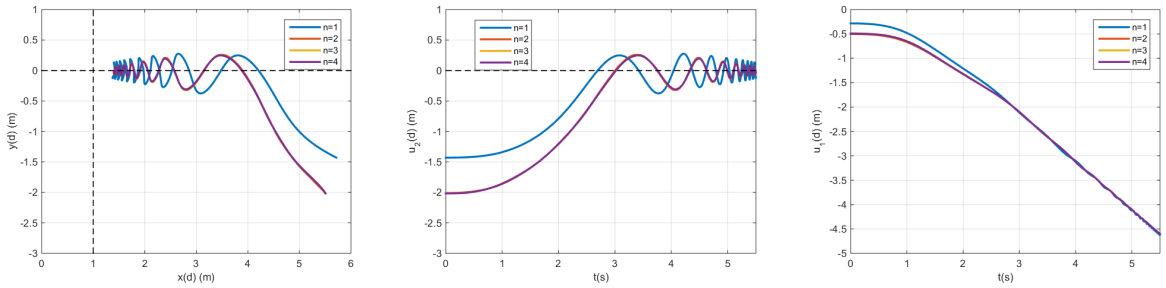

(a) (b) (c)

Figure 4. Example 1: (a): Test of figure 3(a) with $f_+ = 0$N, and $t \mapsto d(t)$, defined by (118). Illustration of the influence of the number of Ritz functions (polynomials) used to reduce the strain fields. (a): Trajectory of the tip rod in the vertical plane. (b,c): Time-evolution of the rod tip displacement: (b) vertical component, (c) horizontal component. All the variables are plotted for $n = 1, 2, 3$ and 4 strain polynomials. The dashed lines indicate the plane of the vertical wall and its normal.

deformed in an uniform density of vertical force $\bar{f}$ (e.g. due to gravity). At $t = 0$, the rod is suddenly retrieved by imposing a time-law for $\ddot{d}$ with a triangular time-profile:

$$\ddot{d}(t) = -2a_0(t/t_f), t \in [0, t_f/2[\ ; \ddot{d}(t) = -2a_0(1 - (t/t_f)), t \in [t_f/2, t_f[\ ; \ddot{d}(t) = 0, t \geq t_f, \tag{118}$$

with $a_0 = 1\text{m.s}^{-2}$, $t_f = 2$s. Here, we use the model of inextensible Kirchhoff rods and only keep the physical parameters: $d(t = 0) = 5$m, $E = 10^7\text{N.m}^{-2}$, $\rho = 10^3\text{kg.m}^{-3}$, $A = 0.2\text{m}^2$, $J_3 = 6.667.10^{-4}\text{m}^4$, $\bar{f} = -200\text{N.m}^{-1}e_2$, of the Reissner rod of [16]. Removing θ, and imposing the time-evolution of $(d, \dot{d}, \ddot{d})$, with (118) in the above numerical algorithm, allows solving $r_{\text{es}}(q, \dot{q}, \ddot{q}, t) = 0$ with (115), at each step of time, under the constraints of the Newmark implicit scheme. The results of this simulation are reported in figures 4, 5 and 6. The reduction of the strain field (here the unique scalar field of curvature $K_3(.)$) is achieved with a basis of monomials of increasing power: $\Phi(s) = (1, s, s^2, ...)$. Figure 4(a), displays the trajectory in the vertical plane of the tip rod $(x, y)(d) = (e_1^T r(d), e_2^T r(d))$ while 4(b,c) display the time-evolution of its vertical and horizontal displacement, i.e. $u_1(d) = e_1^T r(d) - d(t = 0)$ and $u_2(d) = e_2^T r(d)$, for a Ritz basis defined by the first $n = 1, 2, 3$ and 4 monomials. These plots show that the solution has converged with no more than 2 or 3 modes. In all the subsequent tests, we systematically use 4 monomials per scalar strain field. Moreover, one can observe that while the rod slides into the wall, it deforms with oscillations of increasing amplitude and frequency. This nonlinear phenomenon is known as the "slapping effect" of the sliding spaghetti [13]. This effect can be increased by initially bending and releasing the rod. This is illustrated in figure 5, which shows the results obtained for the same rod but subjected to a supplementary tip vertical force $f_+ = -1000e_2$N, which is instantaneously removed at $t = 0$. In figure 6, the same plots are reported but with and without the influence of $(\dot{d}, \ddot{d})(t)$, i.e. with the full dynamic model and with the quasi-steady approximation of "Instance 3" in section 5.2. As this is shown by these plots, neglecting these time-evolutions in the model, drastically changes the results and remove the slapping effects. Finally, note that these results are strongly conditioned by the choice of the internal rod kinematics. Indeed, using Reissner's rod kinematics as in [16], introduces a high shear gradient at the root in the wall, that behaves as a localized elastic joint. This additional compliancy may explain the higher magnitude of deformations, both in statics and dynamics observed in [16]. In more details, with an inextensible Kirchhoff kinematics, the static initial tip displacement is $(u_1, u_2)(d(t = 0)) = (-0.491, -2.017)$m, instead of $(u_1, u_2)(d(t = 0)) = (-0.549, -2.145)$m, with the full Reissner's kinematics, while the amplitude of slapping oscillations is about twice smaller with the Kirchhoff model.

Finally, coming back to remark 8, when we consider the outer piece of rod only, the ODE for d is univocally given by (91) and used by the inverse algorithm, to calculate $Q_{a,d}$ from (112), which involves the transported terms of the original extended Hamilton principle (56). On the other hand, when we consider the entire rod, one uses the ODE (99) as indicated in remark 9, and $Q_{a,d}$ is directly defined as $Q_{a,d} = -N_1(0) = -\mathbb{E}_4^T \Lambda(0)$. As expected, calculating numerically these two expressions of $Q_{a,d}$ for the above tests, shows small negligible discrepancies (about 0.1%), that may be imputed to the numerical integration.

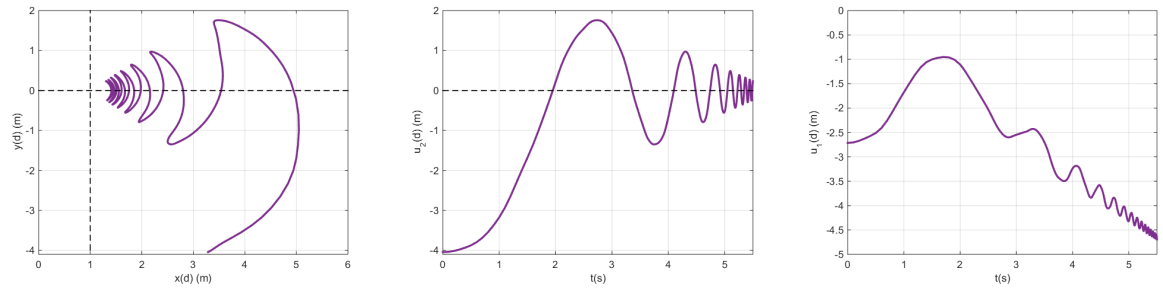

(a) (b) (c)

Figure 5. Example 1: Test of figure 3(a) with $f^+ = -1000e_2$N removed at $t = 0$, and $t \mapsto d(t)$, defined by (118). (a): Trajectory of the tip rod in the vertical plane. (b,c): Time-evolution of the rod tip displacement: (b) vertical component, (c) horizontal component.

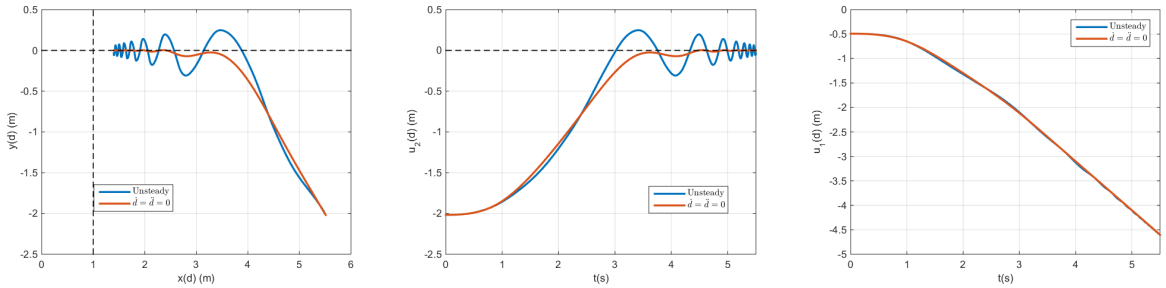

(a) (b) (c)

Figure 6. Example 1: Test of figure 3(a) with $f_+ = 0$N, and $t \mapsto d(t)$, defined by (118). Illustration of the influence of $t \mapsto (\dot{d}, \ddot{d})(t)$. (a): Trajectory of the tip rod in the vertical plane. (b,c): Time-evolution of the rod tip displacement: (b) vertical component, (c) horizontal component. In red color, the unsteady influence of $t \mapsto (\dot{d}, \ddot{d})(t)$ is neglected. In blue color, it is not.

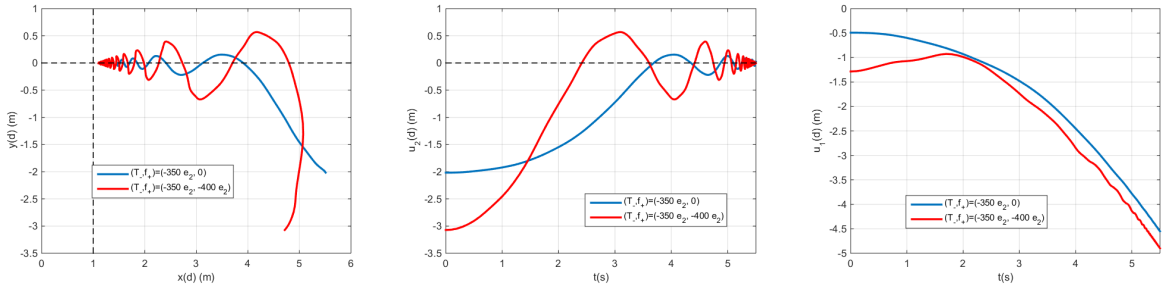

(a) (b) (c)

Figure 7. Example 2: Test of figure 3(b), with $T_- = -350e_2$N applied at $X = 0$, and a tip force $f_+ = 0$N (blue), or $-400e_2$N (red): (a) Trajectory of the tip rod in the vertical plane. (b) Time-evolution of vertical displacement of the end of the beam. (c) Idem for the horizontal displacement.

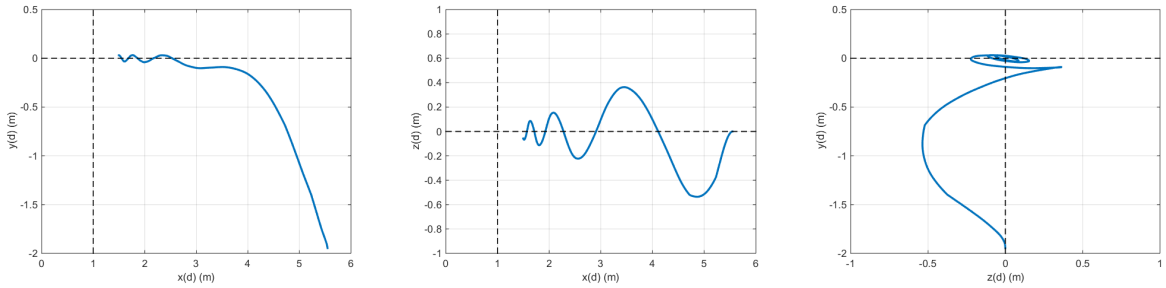

(a) (b) (c)

Figure 8. Example 3: Three dimensional test: Trajectories of the rod tip in the 3 planes (e_1, e_2), (e_1, e_3) and (e_3, e_2). The rod is subjected to a time-constant pulling force and a time-constant rolling torque both applied at the orifice $s = 0$ (i.e., while ignoring the internal piece of rod).

7.2.2. Example 2: "Extended spaghetti problem": 2D retrieval of a sliding rod by imposing a pulling force at $X = 0$

In this second example, we consider the same rod as above, but including the piece inside the wall according to section 6. The rod has a length of $l = 6$m and is initially deployed of $d(t = 0) = 5$m. In this case, the time-evolution of d is no longer imposed by a time-law, but governed by the ODE for d (99), excited at one end by a pulling force T_- of magnitude 350N, and at the other end, by the traction force $N_1(0)$ exerted by the right part of the rod onto the left one across the wall $s = 0$ (see figure 3(b)). As in the previous example, the rod is possibly deformed by an initial load f_+ applied at its free-tip and instantaneously removed at $t = 0$. The motion being restricted to the vertical plane, the rolling field $\theta(.)$ is removed from the model of section 6. To achieve this simulation, we apply the simulation algorithm of remark 9. Denoting the Heaviside function by $H(.)$, the rod is pulled at $t = 0$ by exerting a force $Q_d^\star(t) = N_{ext,1}^{\star-}(t) = -350H(t)$N to the material cross section $X = 0$ ($s = d - l$). Figures 7 (a,b,c) show the trajectory of the rod tip and the time-evolution of its horizontal and vertical displacements both in the case when $f_+ = -400e_2$N and $f_+ = 0$N. Note that in the former case, the rod starts far from its static balance, which creates a strong transitory.

7.2.3. Example 3: 3D retrieval of a sliding-rotating rod by imposing a pulling force and a rolling torque at the orifice in the wall $s = 0$

In figure 8, we report the simulation results of a three-dimensional dynamic test in the conditions of figure 3(b) with $f_+ = 0$N. The rod has a circular cross-section of diameter 0.1155m, with $EJ_2 = EJ_3 = GJ_1 = 1.397 \times 10^3$N.m^2, and $\rho A = 2 \times 10^2$kg.m^{-1}. Its total and initial deployed length are $l = 6$m and $d(t = 0) = 5$m respectively. It is subjected to a vertical spatial density of force $\bar{f} = -40e_2$Nm^{-1}. At $t = 0$s, this rod is suddenly retracted and rotated with a pulling force $Q_d(t) = -50H(t)$N and a rolling torque $Q_\theta(t) = C_{ext,1}^{-}(t) = 5H(t)$Nm, both exerted at its root in the wall. The full strain field $K(.) = (K_1, K_2, K_3)^T(.)$ (curvatures and torsion) are considered and reduced with three monomials $(1, s, s^2, s^3)$ each. Figure 8(a,b,c) shows the time-evolution of the Cartesian coordinates of the rod tip. Note that the slapping effect is now dominant in the horizontal plane, while three-dimensional couplings between bending and torsion, generate normal rotation of the rod with respect to the wall, before entering the guide.

7.2.4. Example 4: 3D deployment and retrieval of a pre-curved rod by imposing a push-pull force at $X = 0$

Like in example 3, we consider the dynamics of the entire rod contained in the two non-material tubes discussed in section 6. However, in contrast to example 3, at $t = 0$, the rod is entirely contained in the inner tube, and pushed with a force $Q_d^\star(t) = N_{ext,1}^{\star-}(t) = 70H(t)$N applied to its left end at $s = d - l$ (or equivalently $X = 0$), while it is free to roll around the guide axis, i.e. $Q_\theta^\star(t) = C_{ext,1}^{\star-}(t) = 0$Nm. The cross-sectional properties of the rod are those of example 3 except that $GJ_1 = +\infty$, i.e. the rod is non-twistable and $K_1(.) = 0$, $K_1^\star(.) = 0$. However, it has a pre-curved shape in 3D defined by $K_{2,o}(X) = (-2X)$rad.m^{-1} and $K_{3,o}(X) = (2X^2 - X)$rad.m^{-1}. In figures 9 and 10, we report the results of a simulation of the extended model of remark 9 applied in these conditions. Figure 9(a) and (b) show the time-evolution

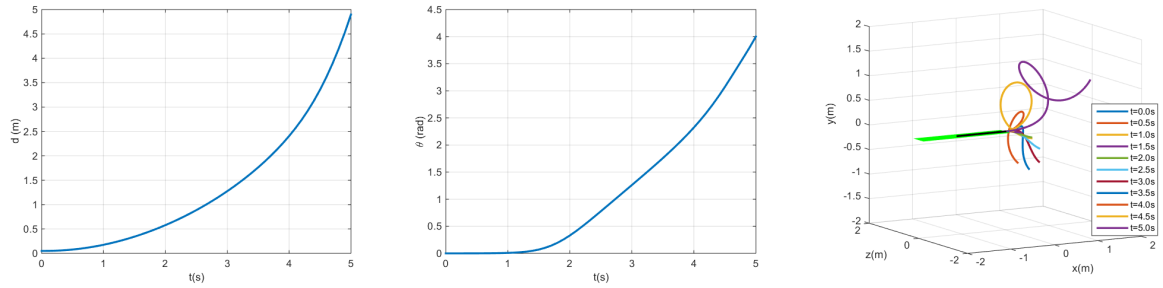

(a) (b) (c)

Figure 9. Example 4: Non-twistable rod deployed out of a wall by pushing it at its material root $X = 0$ with an axial force, while it is free in rolling. (a): Time-evolution of the deployed length d. (b) Time-evolution of the rolling angle θ. Snapshots of the rod every 0.5s.

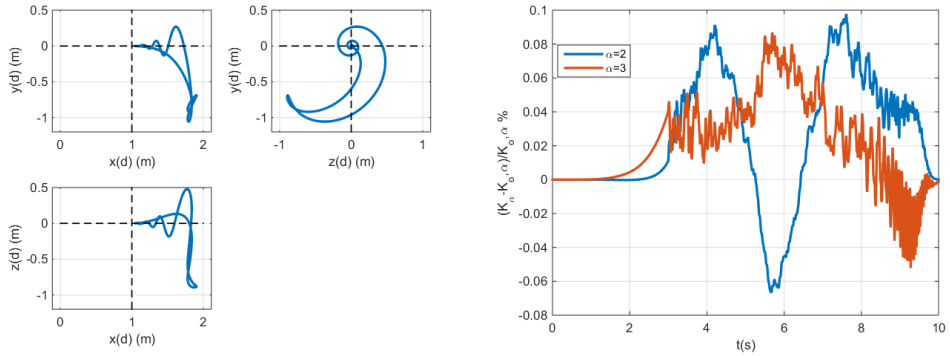

(a) (b)

Figure 10. Example 4: Non-twistable rod pushed and pulled at its material root $X = 0$ with an axial force while it is free of rolling. (a): Trajectory of the tip rod in the three planes of Cartesian space. (b) Time-evolution of the tip value of $((K_2 - K_{2,o})/K_{2,o})(d)$ (blue), and $((K_3 - K_{3,o})/K_{3,o})(d)$ (red).

of d and θ respectively, while snapshots every 0.5s are drawn in figure 9(c). As expected, while deploying outside the guide, the rod recovers its reference shape and rolls freely around the rigid tubular-guide axis. In figure 10, the same test is carried out except that at $t = 3$s, the sign of the push force $Q_d(t)$ is suddenly opposed. The trajectory of the rod tip is plotted in 10(a). The sudden opposition of the push force generates some vibrations as observed in figure 10(b), which displays the time-evolution of $((K_2 - K_{2,o})/K_{2,o})(d)$ and $((K_3 - K_{3,o})/K_{3,o})(d)$.

8. Conclusion

In this paper, we have proposed a method for modeling nonlinear beams sliding through rigid guides. The approach is based on Hamilton's principle and Kirchhoff's inextensible beam model. This kinematics allows to isolate the external part of the sliding rod while allowing to solicit it both in force and motion. To address the problem of non-material boundaries, Hamilton's variational principle was reconsidered from the beginning and adapted to this type of open slender system. The resulting extended principle is none other than the specification of the principle recently proposed by Casseta and Pesce [19], to the case of Cosserat beams. As in this reference, this principle contains some unusual flux terms of Lagrangian density and kinetic momenta across the non-material boundaries. The weak form is deduced from a variational calculus due to Poincaré, which generalizes the usual Lagrangian calculus, from vector spaces to Lie groups (here $SE(3)$). For each non-material domain considered, the application of this calculus leads to a new form of the Cosserat-Poincaré equations adapted to sliding beams, as well as to one Lagrange equation presenting the flux terms of the extended principle. The first of these equations governs the dynamics of the transformations of a non-material beam coincident at each instant with the sliding beam on the non-material domain, the second governs the

dynamics of the sliding degree of freedom. First applied to the sliding spaghetti, this formulation was then extended to its part included in the guide. On the basis of this model, a set of numerical simulations was presented. It is based on a method of resolution inherited from the robotics of rigid poly-articulated systems and recently extended to continuum robots [27]. This numerical method is only based on the rod kinematics and its strong form, considered at each step of time, as some space-ODEs that are integrated forward and backward respectively. These results allow us to reveal the nonlinear behavior of these systems, and especially the well-known slapping phenomenon initially described in Carrier's seminal paper. In the future, we project to apply the approach to deployable slender structures like the non-invasive surgical robots named concentric tube robots (CTR), i.e. continuous robots composed of several pre-bent tubes, nested in each other, and independently pushed and rotated out of a fixed basis [32].

9. Acknowledgment

This work was supported in part by the French National Research Agency (ANR) through the COSSEROOTS research project (2020-2024), in part by the Khalifa University of Science and Technology under Grants RC2-2018-HEIC and CIRA-2020-074..

Appendix A. Proof of (13) and (64)

Performing variational calculus on the Lie group $SE(3)$, requires to use the relations (13) and (64) which link the variation of the twists $\delta\eta$ and $\delta\xi$, to the configuration variation twist $\delta\zeta = (g^{-1}\delta g)^{\vee}$, before proceeding to the usual by part integration in time and space, and to deduce the expected motion equations. These key relations between variations are named "commutation relations" in the article, since they fix the rules of exchange between the differential operators $\delta.$, $\partial./\partial t$ and $\partial./\partial X$ in the material context of (13), and $\delta.$, $\partial./\partial t$ and $\partial./\partial s$, in the non-material context of (64). To illustrate the derivation of these relations, one can consider the material case only, since similar arguments with s instead of X, hold for the non-material one. In this case, let us first remark that since variations $\delta.$ are imposed at t and X fixed, one has the symmetry of second order derivatives of transformations:

$$\delta\partial_t g = \partial_t \delta g \ , \ \delta\partial_X g = \partial_X \delta g. \tag{A.1}$$

Then, using the definitions of $\delta\zeta$, η and ξ in terms of g, namely $\delta g = g\delta\hat{\zeta}$, $\partial_t g = g\hat{\eta}$, and $\partial_X g = g\hat{\xi}$ in the two relations of (A.1), gives the expected relations (13). To be convinced of this, let us consider the first of them, we have then:

$$\delta(g\hat{\eta}) = \partial_t(g\delta\hat{\zeta}) \ \Leftrightarrow \ \delta g\hat{\eta} + g\delta\hat{\eta} = \partial_t g\delta\hat{\zeta} + g\partial_t\delta\hat{\zeta}, \tag{A.2}$$

and so, using once more the definitions $\delta g = g\delta\hat{\zeta}$ and $\partial_t g = g\hat{\eta}$, one finds:

$$g(\delta\hat{\zeta}\hat{\eta} + \delta\hat{\eta}) = g(\hat{\eta}\delta\hat{\zeta} + \partial_t\delta\hat{\zeta}), \tag{A.3}$$

which holding for any g, leads to:

$$\delta\hat{\eta} = \partial_t\delta\hat{\zeta} + \hat{\eta}\delta\hat{\zeta} - \delta\hat{\zeta}\hat{\eta} = \partial_t\delta\hat{\zeta} + [\hat{\eta}, \delta\hat{\zeta}]. \tag{A.4}$$

Finally using the anti-hat ($\vee$) operation of section 2 with (6), provides the first of the commutation relation in terms of twists of (13), while the second is derived in a similar way by replacing t by X. These commutation relations were first proposed by Poincaré in his note of 1901 [23] for any Lie group, and have since then, been used extensively in the literature on the geometrically exact finite elements method of [12], [26] for the Lie group $SO(3)$ and more recently by [20], [33] for $SE(3)$. Remarkably, all the ad operators appearing in the expressions of the article have for unique origin these commutation relations.

Appendix B. Proof of (56)

The proof of (56) is presented in this appendix. It starts by restating a key relation between the variation of the Lagrangian and the virtual work of kinetic momentum and external forces in the Lagrangian setting, i.e. with the material variable X. This relation is the very last step before stating the usual Hamilton principle of a closed Cosserat rod system from d'Alembert's principle [34]. To extend Hamilton's principle from closed to open Cosserat rod systems, one needs to apply Reynolds transport theorem twice to this relation, once with the real velocity field (48), and once more with the virtual one, in the form of (51). The first application of this theorem leads to the extended Hamilton principle of [11], here specialized to a Cosserat rod. The second was more recently proved to be necessary when the velocity of the non-material boundaries depends on the configuration of the isolated system [19]. Note that the same extension of Hamilton's principle, with all the transported terms, has been proposed in [20] for modelling swimming of a slender body in order to revisit the large amplitude elongated body theory by Lighthill [35].

Appendix B.1. First step of the proof

In this first step, as in the section 2 of the article, all the fields depend on the material label X which runs over a fixed material domain $[0, l]$, where l is the length of the rod. Considering a Cosserat rod of Lagrangian $L = T - U = \int_0^l \mathfrak{L}\, dX = \int_0^l \mathfrak{T} - \mathfrak{U}\, dX$, with $\mathfrak{T}$ and $\mathfrak{U}$ the density of kinetic and strain energy densities, we first want to prove that we have:

$$\delta L = \frac{\partial}{\partial t}\int_0^l \delta\zeta^T \left(\frac{\partial \mathfrak{T}}{\partial \eta}\right) dX - \delta W_{ext}, \tag{B.1}$$

where δW_{ext} is the virtual work of the external load. To prove this relation, we start by stating d'Alembert's principle of virtual work which in this case, holds for all $\delta\zeta(.)$ following the material cross-sections, and compatible with the geometric BCs:

$$\delta W_{acc} = \int_0^l \delta\zeta^T \left(\frac{\partial}{\partial t}\left(\frac{\partial \mathfrak{T}}{\partial \eta}\right) - ad_\eta^T\left(\frac{\partial \mathfrak{T}}{\partial \eta}\right)\right) dX = \delta W_{ext} - \delta U, \tag{B.2}$$

where δW_{acc} and $-\delta U$, are respectively, the virtual work of the acceleration amounts and that of the internal forces, which are assumed to be conservative. To progress further, note that δW_{acc} can be rewritten as:

$$\delta W_{acc} = \frac{\partial}{\partial t}\int_0^l \delta\zeta^T \left(\frac{\partial \mathfrak{T}}{\partial \eta}\right) dX - \int_0^l \delta\zeta^T ad_\eta^T\left(\frac{\partial \mathfrak{T}}{\partial \eta}\right) + \left(\frac{\partial \delta\zeta^T}{\partial t}\frac{\partial \mathfrak{T}}{\partial \eta}\right) dX. \tag{B.3}$$

Then using the time-variation commutation relation (13), allows (B.3) to be rewritten as:

$$\delta W_{acc} = \frac{\partial}{\partial t}\int_0^l \delta\zeta^T \left(\frac{\partial \mathfrak{T}}{\partial \eta}\right) dX - \int_0^l \delta\zeta^T ad_\eta^T\left(\frac{\partial \mathfrak{T}}{\partial \eta}\right) + (\delta\eta^T - \delta\zeta^T ad_\eta^T)\left(\frac{\partial \mathfrak{T}}{\partial \eta}\right) dX,$$

which after simplifications, becomes:

$$\delta W_{acc} = \frac{\partial}{\partial t}\int_0^l \delta\zeta^T \left(\frac{\partial \mathfrak{T}}{\partial \eta}\right) dX - \int_0^l \delta\eta^T \left(\frac{\partial \mathfrak{T}}{\partial \eta}\right) dX = \frac{\partial}{\partial t}\int_0^l \delta\zeta^T \left(\frac{\partial \mathfrak{T}}{\partial \eta}\right) dX - \delta T.$$

Using this expression of δW_{acc} in the weak-form (B.2), gives:

$$\delta W_{acc} = \frac{\partial}{\partial t}\int_0^l \delta\zeta^T \left(\frac{\partial \mathfrak{T}}{\partial \eta}\right) dX - \delta T = \delta W_{ext} - \delta U, \tag{B.4}$$

which finally gives (B.1), and concludes the first step of the proof.

Appendix B.2. Second step of the proof

Remark that in (B.1), $\partial/\partial t = \partial_t$, and δ, stand for the Lagrangian time derivation and Lagrangian variation (or virtual time derivation), which therefore follow the material particles in their real and virtual motion respectively. Now, let us consider an open system constituted by the piece of our sliding Cosserat rod $[\underline{X}, l]$, outside of the wall (figure 1). We define the non-material variable $s \in [0, d]$ which runs over the non-material tube enclosing this piece of rod at each time. If the field of pause of this piece of rod is parameterized by $g(.) : s \in [0, d] \mapsto g(s) \in SE(3)$, we need to rewrite (B.1) with $[0, l]$ replaced by $[\underline{X}, l]$, in the alternative non-material form:

$$\Delta L = \frac{D}{Dt} \int_0^d \Delta\zeta^T \left(\frac{\partial \mathfrak{T}}{\partial \eta_D} \right) ds - \Delta W_{ext}, \tag{B.5}$$

where D/Dt and Δ denote the total derivative and the total variation of any function of the non-material variable s. Applying the Reynolds transport theorem (48) to the density $\Delta\zeta^T(\partial\mathfrak{T}/\partial\eta_D)$, gives:

$$\frac{D}{Dt} \int_0^d \Delta\zeta^T \left(\frac{\partial \mathfrak{T}}{\partial \eta_D} \right) ds = \frac{d}{dt} \int_0^d \Delta\zeta^T \left(\frac{\partial \mathfrak{T}}{\partial \eta_D} \right) ds + \left[\Delta\zeta^T \left(\frac{\partial \mathfrak{T}}{\partial \eta_D} \right) \right]_0^d \dot{d}. \tag{B.6}$$

Then, introducing (B.6) into (B.5) gives after time-integration between t_a and t_b:

$$\int_{t_a}^{t_b} \Delta L \, dt = \int_{t_a}^{t_b} \left(\left[\Delta\zeta^T \left(\frac{\partial \mathfrak{T}}{\partial \eta_D} \right) \right]_0^d \dot{d} - \Delta W_{ext} \right) dt, \tag{B.7}$$

where we used the fact that the variation being applied while maintaining the configuration fixed at $t = t_a$ and $t = t_b$, we have $\Delta\zeta(., t_a) = \Delta\zeta(., t_b) = 0$. This ends the second step of the proof.

Appendix B.3. Third step of the proof

We now consider the left hand side member of (B.7). As in [20], one can apply the Reynolds theorem (51) to the Lagrangian density $\mathfrak{L}$. This gives:

$$\Delta L = \Delta \int_0^d \mathfrak{L} \, ds = \int_0^d \delta\mathfrak{L} \, ds + [\mathfrak{L}]_0^d \, \delta d. \tag{B.8}$$

Finally, introducing (B.8) into (B.7) concludes the proof of (56).

References

[1] L.-Q. Chen, Analysis and control of transverse vibrations of axially moving strings, Applied Mechanical Review 58 (2) (2005) 91–116.

[2] M. Gürgöze, S. Yüksel, Transverse vibrations of a flexible beam sliding through a prismatic joint, Journal of Sound and Vibration 223 (3) (1999) 467–482. doi:https://doi.org/10.1006/jsvi.1999.2155.

[3] K. Miura, Concepts of deployable space structures, International Journal of Space Structures 8 (1-2) (1993) 3–16.

[4] G. F. Carrier, The spaghetti problem, Am. Math. Monthly 56 (1) (1949) 669–672.

[5] M. Stylianou, B. Tabarrok, Finite element analysis of an axially moving beam, part i: Time integration, Journal of Sound and Vibration 178 (4) (1994) 433 – 453. doi:https://doi.org/10.1006/jsvi.1994.1497.

[6] M. Stylianou, B. Tabarrok, Finite element analysis of an axially moving beam, part ii: Stability analysis, Journal of Sound and Vibration 178 (4) (1994) 455 – 481. doi:https://doi.org/10.1006/jsvi.1994.1498.

[7] R. Theodore, J. Arakeri, J. Ghosal, The modelling of axially translating flexible beams, Journal of Sound and Vibration 191 (3) (1996) 363 – 376. doi:https://doi.org/10.1006/jsvi.1996.0128.

[8] B. Tabarrok, C. Leech, Y. Kim, On the dynamics of an axially moving beam, J. Franklin Inst. 297 (3) (1974) 201–220.

[9] K. Behdinan, J. Stylianou, B. Tabarrok, Dynamics of flexible sliding beams — non-linear analysis part i: Formulation, Journal of Sound and Vibration 208 (4) (1997) 517 – 539. doi:https://doi.org/10.1006/jsvi.1997.1167.

[10] K. Behdinan, B. Tabarrok, Dynamics of flexible sliding beams — non-linear analysis part ii: Transient response, Journal of Sound and Vibration 208 (4) (1997) 541 – 565. doi:https://doi.org/10.1006/jsvi.1997.1168.

[11] D. McIver, Hamilton's principle for systems of changing mass, Journal of Engineering Mathematics 7 (3) (1973) 249–261.

[12] J. Simo, A finite strain beam formulation. the three-dimensional dynamic problem. part i, Computer Methods in Applied Mechanics and Engineering 49 (1) (1985) 55 – 70.

[13] L. Vu-Quoc, S. Li, Dynamics of sliding geometrically-exact beams: large angle maneuver and parametric resonance, Comput. Methods Appl. Mech. Engrg. 120 (4) (1995) 65–118.

[14] A. Donea, J. P. Ponthot, A. Rodriguez-Ferran, Encyclopedia of Computational Mechanics Volume 1: Fundamentals, Wiley, Amsterdam, 2004, Ch. Arbitrary Lagrangian–Eulerian methods, p. 14.
[15] A. Humer, Dynamic modeling of beams with non-material, deformation-dependent boundary conditions, Journal of Sound and Vibration 332 (3) (2013) 622–641. doi:https://doi.org/10.1016/j.jsv.2012.08.026.
[16] I. Steinbrecher, A. Humer, L. Vu-Quoc, On the numerical modeling of sliding beams: A comparison of different approaches, Journal of Sound and Vibration 408 (2017) 270 – 290. doi:https://doi.org/10.1016/j.jsv.2017.07.010.
[17] A. Humer, I. Steinbrecher, L. Vu-Quoc, General sliding-beam formulation: A non-material description for analysis of sliding structures and axially moving beams, Journal of Sound and Vibration 480 (2020) 115341. doi:https://doi.org/10.1016/j.jsv.2020.115341.
[18] E. Reissner, On a one-dimensional large displacement finite-strain beam theory, Studies in Applied Mathematics 52 (2) (1973) 87–95.
[19] L. Casetta, C. Pesce, The generalized hamilton's principle for a non-material volume, Acta Mech 224 (1) (2013) 919–924.
[20] F. Boyer, M. Porez, A. Leroyer, Poincaré - cosserat equations for the lighthill three-dimensional large amplitude elongated body theory: Application to robotics, Journal of Nonlinear Science 20 (1) (2010) 47–79.
[21] J. Lighthill, Mathematical Biofluiddynamics, Society for Industrial and Applied Mathematics,U.S., 1987.
[22] F. Boyer, F. Renda, Poincaré's equations for cosserat media: Application to shells, Journal of Nonlinear Science 27 (1) (2016) 1–44. doi:10.1007/s00332-016-9324-7.
[23] H. Poincaré, Sur une forme nouvelle des equations de la mecanique, Compte Rendu de l'Academie des Sciences de Paris 132 (1901) 369 – 371.
[24] V. I. Arnold, Mathematical Methods of Classical Mechanics, Springer, New York, 1989.
[25] J. E. Marsden, T. S. Ratiu, Introduction to Mechanics and Symmetry, 2nd Edition, Springer-Verlag, 1999.
[26] J. C. Simo, L. Vu-Quoc, On the dynamics in space of rods undergoing large motions - a geometrically exact approach, Computer Methods in Applied Mechanics and Engineering 66 (2) (1988) 125 – 161.
[27] F. Boyer, V. Lebastard, F. Candelier, F. Renda, Dynamics of continuum and soft robots: A strain parameterization based approach, IEEE Transactions on Robotics (2020) 1–17doi:10.1109/TRO.2020.3036618.
[28] S. S. Antman, Ordinary differential equations of nonlinear elasticity i: Foundations of the theories of non-linearly elastic rods and shell, Arch. Rat. Mech. Anal. 61 (4) (1976) 307–351.
[29] J. Ericksen, C. Truesdell, Exact theory of stress and strain in rods and shells., Archive for Rational Mechanics and Analysis 1 (1) (1958) 295–323. doi:10.1007/s00332-016-9324-7.
[30] A. R. Plastino, J. C. Muzzio, On the use and abuse of newton's second law for variable mass problems, Celestial Mechanics and Dynamical Astronomy 53 (3) (1992) 227–232.
[31] N. A. Faruk Senan, O. M. O'Reilly, T. N. Tresierras, Modeling the growth and branching of plants: A simple rod-based model, Journal of the Mechanics and Physics of Solids 56 (10) (2008) 3021 – 3036. doi:https://doi.org/10.1016/j.jmps.2008.06.005.
[32] V. Till, J.and Aloi, K. E. Riojas, P. L. Anderson, R. J. Webster III, C. Rucker, A dynamic model for concentric tube robots, IEEE Transactions on Robotics 36 (6) (2020) 1704–1718. doi:10.1109/TRO.2020.3000290.
[33] V. Sonneville, A. Cardona, O. Bruls, Geometrically exact beam finite element formulated on the special euclidean group se(3), Comput. Methods Appl. Mech. Engrg. 268 (2014) 451–474.
[34] L. Meirovitch, Methods of Analytical Dynamics, McGraw-Hill, New York, 1970.
[35] J. Lighthill, Large-amplitude elongated-body theory of fish locomotion, Proceedings of the Royal Society of London. Series B, Biological Sciences 179 (1055) (1971) 125–138.